Spectroscopy of selected T Tauri stars

Ľubomír Hambálek
with: T. Pribulla, M. Vaňko, and E. Kundra

June 17, 2023

T Tauri stars

Young (Li I 6707Å absorption), lower mass (0.5-2.5 $M_\odot$), usually binaries

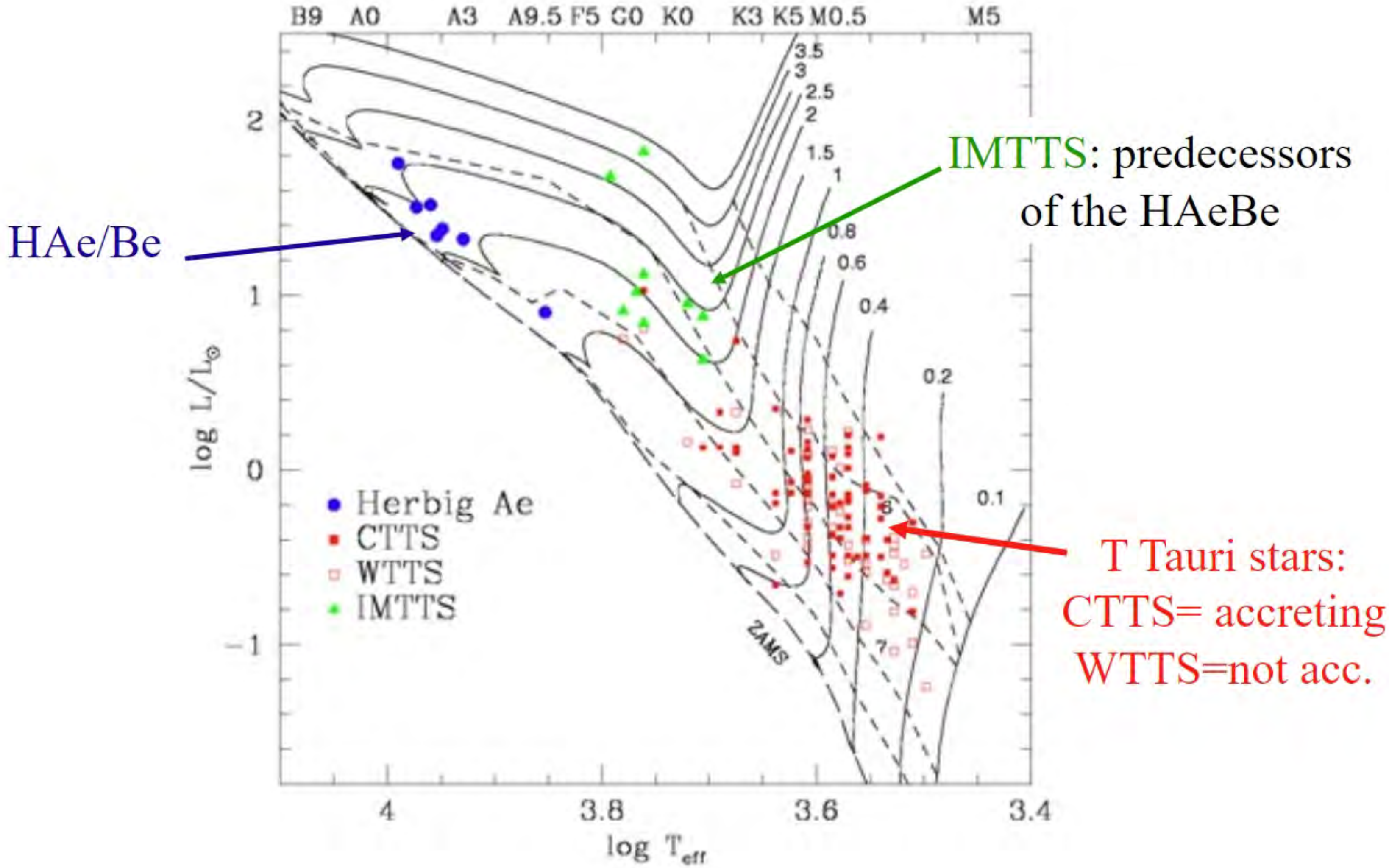

T Tauri stars

„Classical“
- EW H_α > 10 Å
- NIR excess – accretion disk
- jets and outflows
- magnetic disk interaction

„Weak-lined“
- EW H_α < 10 Å
- almost no NIR excess – dissipated disk
- no jets or outflows
- solar-type magnetic activity

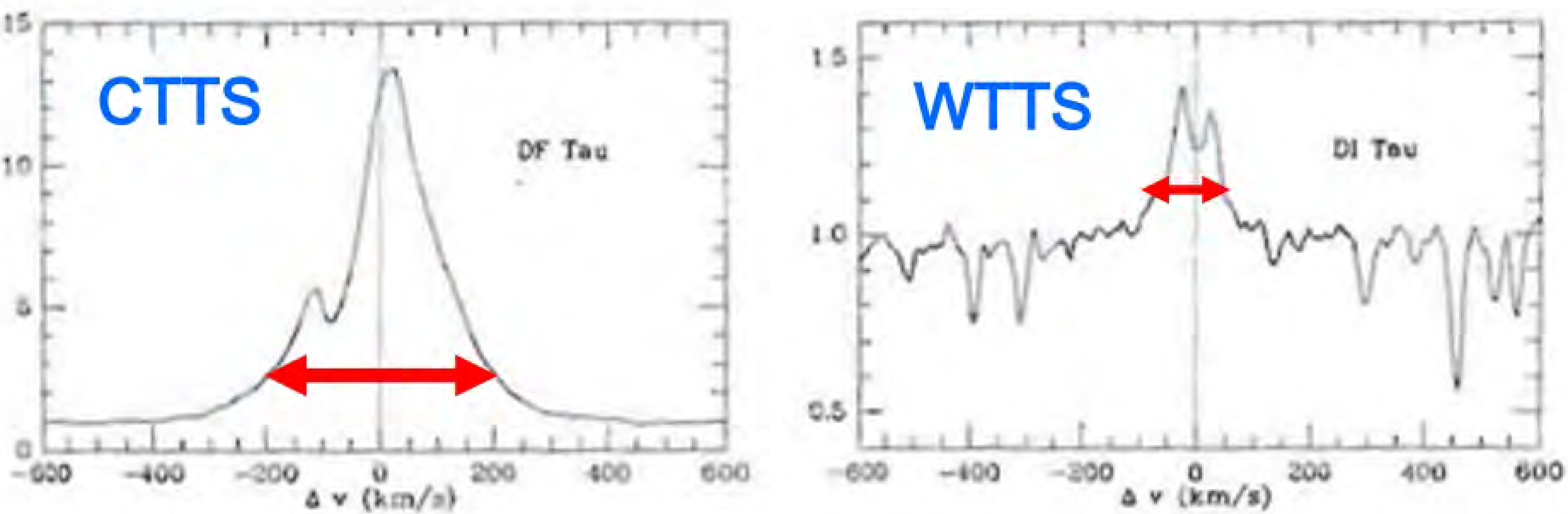

Lee Hartmann, 2000

T Tauri stars

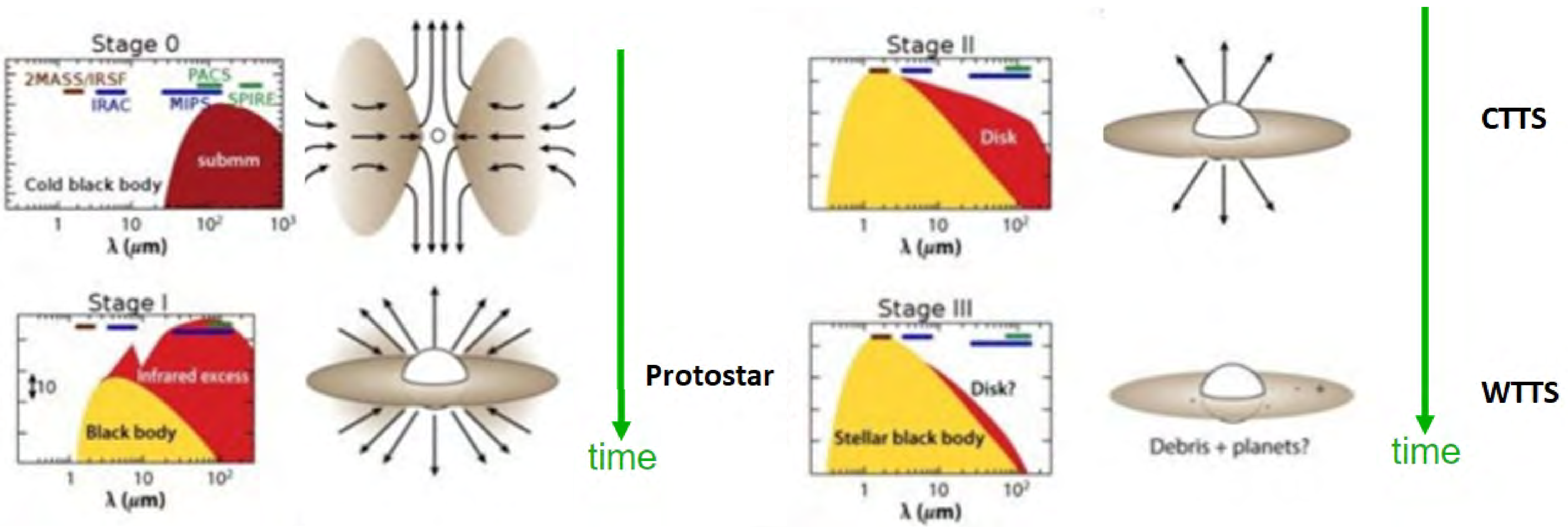

Taurus-Auriga star forming region

Nearest SFR (~140 pc), Ø ~30 pc

$M_{\mathrm{total}} \sim 3.5\times10^4\ M_\odot$

Our sample:

V < 11 mag WTTS

with unknown/contradicting parameters in literature.

#	star name	this	N12	K17	N95	W07	W96
01	HD 285281	K0 V	K0	F9	K0	K1	K1
02	BD+19 656	K1 V	K1	K1.5	G0		K1
03	HD 284135	G2 V	G0	G3	G0	G3 V	G3
04	HD 284149	F9 V	F8	G1	G0		G1
05	HD 281691	K0 V	G8	K2.5	G5	G8 III	K1
06	HD 284266	G9 V	K0	K0	F8	K0 V	K0
08	HD 284503	G2 V	G8	G8	G0		G8
09	HD 284496	G8 V	G0	K0	G0		K0
12	HD 283798	G2 IV	G2	G7	G5		G7
13	HD 283782	G2 IV		K1	K0		K1
14	HD 030171	G3 IV	G5	G3			G5
15	HD 031281	G2 V	G0	G1		G1 V	G1
16	HD 286179	G2 V	G0	G3	G0	G3 V	G3
17	HD 286178	K0 V	K1	K1	G5		K1
18	HD 283447	K2 V	K3		K2		
19	HD 283572	G2 IV	G2	G4	G0		
20	HD 285778	G7 V	K1	G6	G0		
21	HD 283518	K3 V	K7	K3	K5		

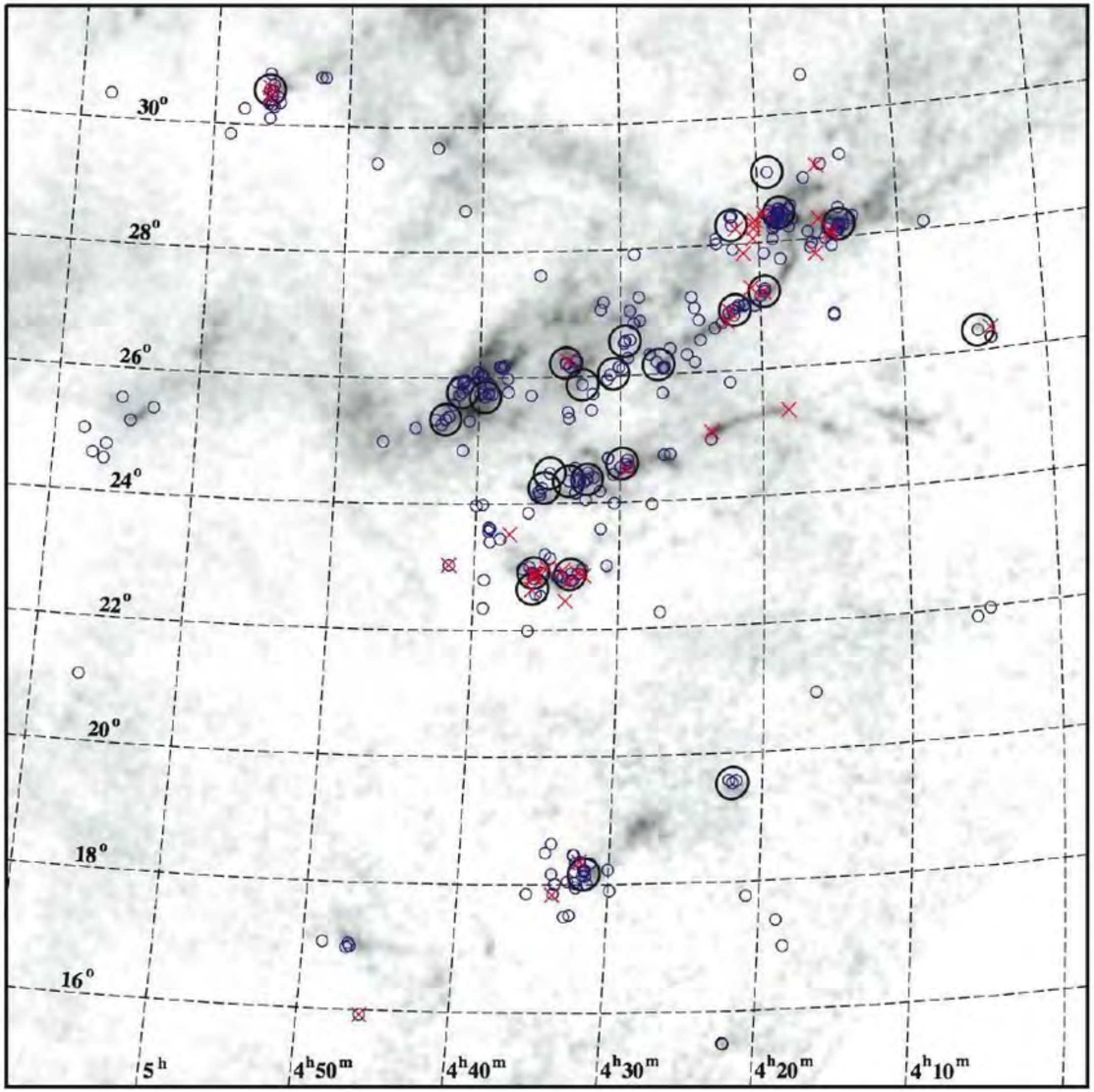

Mamajek, 2009

Spectra

Continuation of previous photometric research of these objects (see Hambálek, et al. 2019)

Tautenburg (TLS, Germany), Skalanté Pleso (SP, Slovakia), Stará Lesná (SL, Slovakia), and Asiago (ASI, Italy)

Site	Telescope	*R*	# objects	# spectra	Season	
TLS-DE	2.0 m	31 500	20	70	2017	
SP-SK	1.3 m	38 000	4	4	2016-2018	
SL-SK	0.6 m	11 000	21	80	2015-2017	
			15	40	2022	
ASI-IT	1.2 m	1 200	18	18	2018	+Ca II H&K
				Σ 212		

Radial velocities and EW

RV templates: K2V (HD 03765), K0V (HD 23169), and G2V (HD 65583) with v_{rot} < 10 km.s^{-1}

Table 3. Measured mean values of radial velocities, rotational line broadening, heliocentric velocities, and EWs of selected lines (in columns 8 – 12). In the case of sodium lines, only the interstellar absorption profile was measured. For HD 283447, the total EW of twin ISM peaks was used (see Figure 4).

TTS	Object name	*RV* [km s^{-1}]	*v* sin *i* [km s^{-1}]	*U* [km s^{-1}]	*V* [km s^{-1}]	*W* [km s^{-1}]	Hα [mÅ]	Li 6104 [mÅ]	Li 6708 [mÅ]	Na 5890 [mÅ]	Na 5896 [mÅ]
01	HD 285281	+14.01	80.0	−12.04	−5.92	−9.27	-	370(21)	423(8)	70(5)	73(5)
02	V1298 Tau	+10.99	38.8	−9.49	−6.63	−7.81	254(19)	383(20)	376(16)	-	-
03	HD 284135	+14.81	72.6	−13.5	−7.3	−9.51	824(21)	243(15)	193(15)	71(4)	74(4)
04	HD 284149	+15.82	28.4	−14.23	−6.61	−9.09	720(16)	222(13)	169(11)	33(5)	13(5)
05	HD 281691	+11.22	22.4	−13.66	−17.65	−8.21	145(15)	369(17)	344(13)	-	-
06	HD 284266	+14.83	33.0	−12.10	−5.88	−9.00	408(20)	295(18)	239(15)	147(7)	30(7)
07	HIP 20782	+16.96	50.3	−13.36	−8.31	−13.31	-	238(18)	172(18)	9(5)	4(5)
08	HD 284503	+14.82	42.8	−16.03	−21.04	−3.67	125(16)	306(15)	274 (14)	32(5)	20(4)
09	HD 284496	+15.25	25.0	−13.33	−6.02	−9.86	297(18)	345(18)	288(14)	70(11)	31(11)
10	HD 285840	+20.96	25.7	−18.61	−3.15	−10.54	-	345(18)	214(14)	-	-
11	HD 285957	+17.21	25.8	−15.10	−16.11	−7.27	155(15)	377(18)	411(14)	30(6)	52(6)
12	HD 283798	+12.96	26.5	−11.81	−6.88	−10.50	380(30)	305(13)	243(11)	-	-
13	HD 283782	+17.90	79.5	−17.48	−20.53	−15.33	−3937(15)	245(19)	237(20)	126(6)	117(6)
14	HD 30171	+18.71	112.9	−16.77	−16.69	−6.30	706(27)	269(23)	273(9)	76(6)	68(6)
15	HD 31281	+15.03	84.9	−12.47	−7.16	−10.33	970(18)	233(15)	167(5)	71(4)	68(4)
16	HD 286179	+12.51	16.5	−10.32	−4.25	−7.73	1316(17)	247(16)	167(11)	-	-
17	HD 286178	+18.85	46.6	−16.54	−16.79	−5.67	211(17)	384(16)	416(15)	51(6)	45(5)
18	HD 283447	+3.55	42.7	−3.73	−13.15	−9.31	−1397(22)	386(20)	500(18)	108(11)*	144(11)*
19	HD 283572	+15.51	81.9	−15.57	−12.18	−11.17	899(15)	256(13)	274(14)	82(3)	67(3)
20	HD 285778	+15.19	17.5	−12.83	−6.29	−9.40	510(18)	295(16)	269(11)	-	-
21	HD 283518	+18.46	70.9	−18.41	−11.07	−11.81	−154(25)	394(26)	517(26)	17(9)	9(9)

* = found a quadruple star, multiple absorptions in sodium profile, see text.

Radial velocities and EW

RV templates: K2V (HD 03765), K0V (HD 23169), and G2V (HD 65583) with v_{rot} < 10 km.s^{-1}

Table 3. Measured mean values of radial velocities, rotational line broadening, heliocentric velocities, and EWs of selected lines (in columns 8 – 12). In the case of sodium lines, only the interstellar absorption profile was measured. For HD 283447, the total EW of twin ISM peaks was used (see Figure 4).

TTS	Object name	*RV* [km s^{-1}]	*v* sin *i* [km s^{-1}]	*U* [km s^{-1}]	*V* [km s^{-1}]	*W* [km s^{-1}]	Hα [mÅ]	Li 6104 [mÅ]	Li 6708 [mÅ]	Na 5890 [mÅ]	Na 5896 [mÅ]
01	HD 285281	+14.01	80.0	−12.04	−5.92	−9.27	-	370(21)	423(8)	70(5)	73(5)
02	V1298 Tau	+10.99	38.8	−9.49	−6.63	−7.81	254(19)	383(20)	376(16)	-	-
03	HD 284135	+14.81	72.6	−13.5	−7.3	−9.51	824(21)	243(15)	193(15)	71(4)	74(4)
04	HD 284149	+15.82	28.4	−14.23	−6.61	−9.09	720(16)	222(13)	169(11)	33(5)	13(5)
05	HD 281691	+11.22	22.4	−13.66	−17.65	−8.21	145(15)	369(17)	344(13)	-	-
06	HD 284266	+14.83	33.0	−12.10	−5.88	−9.00	408(20)	295(18)	239(15)	147(7)	30(7)
07	HIP 20782	+16.96	50.3	−13.36	−8.31	−13.31	-	238(18)	172(18)	9(5)	4(5)
08	HD 284503	+14.82	42.8	−16.03	−21.04	−3.67	125(16)	306(15)	274 (14)	32(5)	20(4)
09	HD 284496	+15.25	25.0	−13.33	−6.02	−9.86	297(18)	345(18)	288(14)	70(11)	31(11)
10	HD 285840	+20.96	25.7	−18.61	−3.15	−10.54	-	345(18)	214(14)	-	-
11	HD 285957	+17.21	25.8	−15.10	−16.11	−7.27	155(15)	377(18)	411(14)	30(6)	52(6)
12	HD 283798	+12.96	26.5	−11.81	−6.88	−10.50	380(30)	305(13)	243(11)	-	-
13	HD 283782	+17.90	79.5	−17.48	−20.53	−15.33	−3937(15)	245(19)	237(20)	126(6)	117(6)
14	HD 30171	+18.71	112.9	−16.77	−16.69	−6.30	706(27)	269(23)	273(9)	76(6)	68(6)
15	HD 31281	+15.03	84.9	−12.47	−7.16	−10.33	970(18)	233(15)	167(5)	71(4)	68(4)
16	HD 286179	+12.51	16.5	−10.32	−4.25	−7.73	1316(17)	247(16)	167(11)	-	-
17	HD 286178	+18.85	46.6	−16.54	−16.79	−5.67	211(17)	384(16)	416(15)	51(6)	45(5)
18	HD 283447	+3.55	42.7	−3.73	−13.15	−9.31	−1397(22)	386(20)	500(18)	108(11)*	144(11)*
19	HD 283572	+15.51	81.9	−15.57	−12.18	−11.17	899(15)	256(13)	274(14)	82(3)	67(3)
20	HD 285778	+15.19	17.5	−12.83	−6.29	−9.40	510(18)	295(16)	269(11)	-	-
21	HD 283518	+18.46	70.9	−18.41	−11.07	−11.81	−154(25)	394(26)	517(26)	17(9)	9(9)

* = found a quadruple star, multiple absorptions in sodium profile, see text.

Atmospheric modelling

`iSpec` software by Blanco-Cuaresma et al., 2014

- corrected RV prior modelling, checked with respect to telluric lines
- fitting region: 4 800 – 6 800 Å – Balmer
- VALD line list (Kupka et al., 2011)
- library of artificial spectra convolved to current R
- initial values from previous paper (Hambálek, et al., 2019)
- runs with different starting point
- visual check of fits of Mg I triplet
- Na I doublet and other lines

Parameter	Range	
$T_{\rm eff}$ [K]	3500 ... 6000	
$\log g$	2.5 ... 5.0	
[Fe/H]	−1.0 ... +0.5	
[α/Fe]	0.0	fixed
$v \sin i$ [km s^{-1}]	adopted from BF	fixed
ξ [km s^{-1}]	1.05	
u	0.6	fixed
R	11 500, 31 500, 38 000	fixed

Atmospheric modelling

- correlation of T_{eff} and log g
- errors from iSpec as sigma
- bi-directional Gaussian

$$E_T = \exp\left(-\frac{(T - T_0)^2}{2\sigma_T^2(1 - C^2)}\right), E_{\log g} = \exp\left(-\frac{([\log g] - [\log g_0])^2}{2\sigma_g^2(1 - C^2)}\right)$$

- with cross-correlation term

$$E_C = \exp\left(C\frac{(T - T_0)([\log g] - [\log g_0])}{\sigma_T \sigma_g (1 - C^2)}\right)$$

- final function with normalization

$$A \times E_T \times E_{\log g} \times E_C, A = \frac{1}{2\pi\sigma_T\sigma_g\sqrt{1 - C^2}}$$

Atmospheric modelling

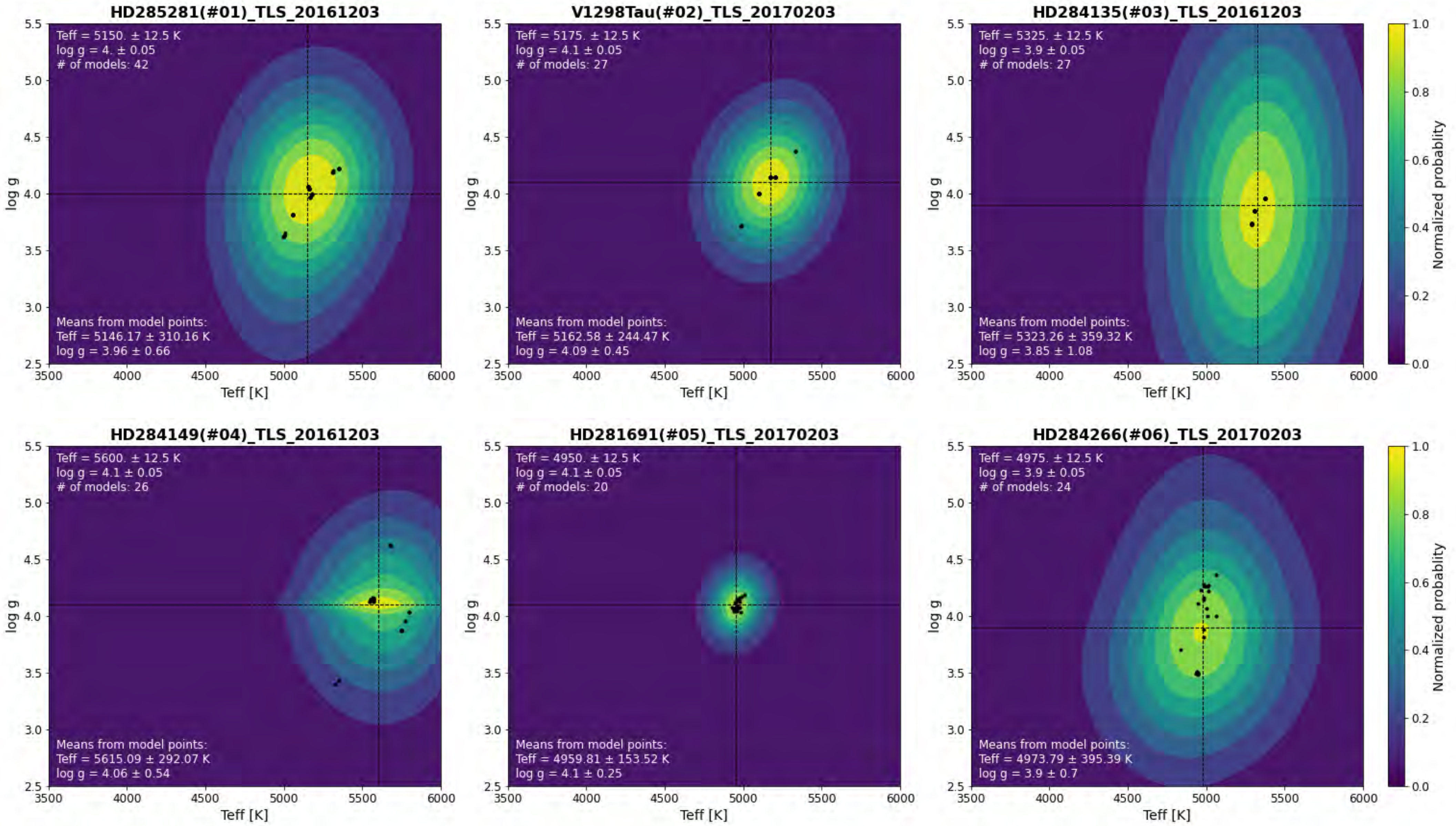

Atmospheric modelling

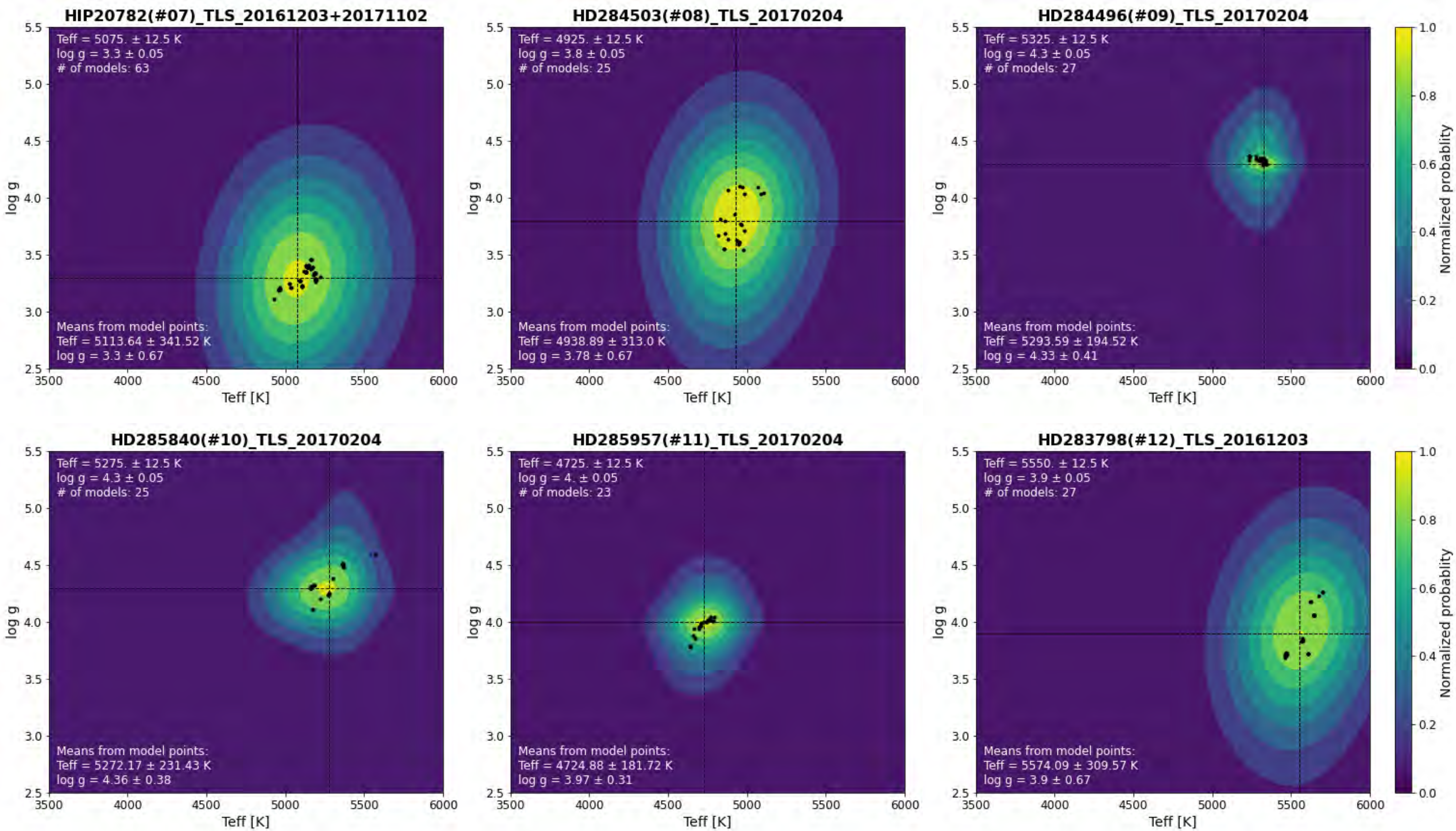

Atmospheric modelling

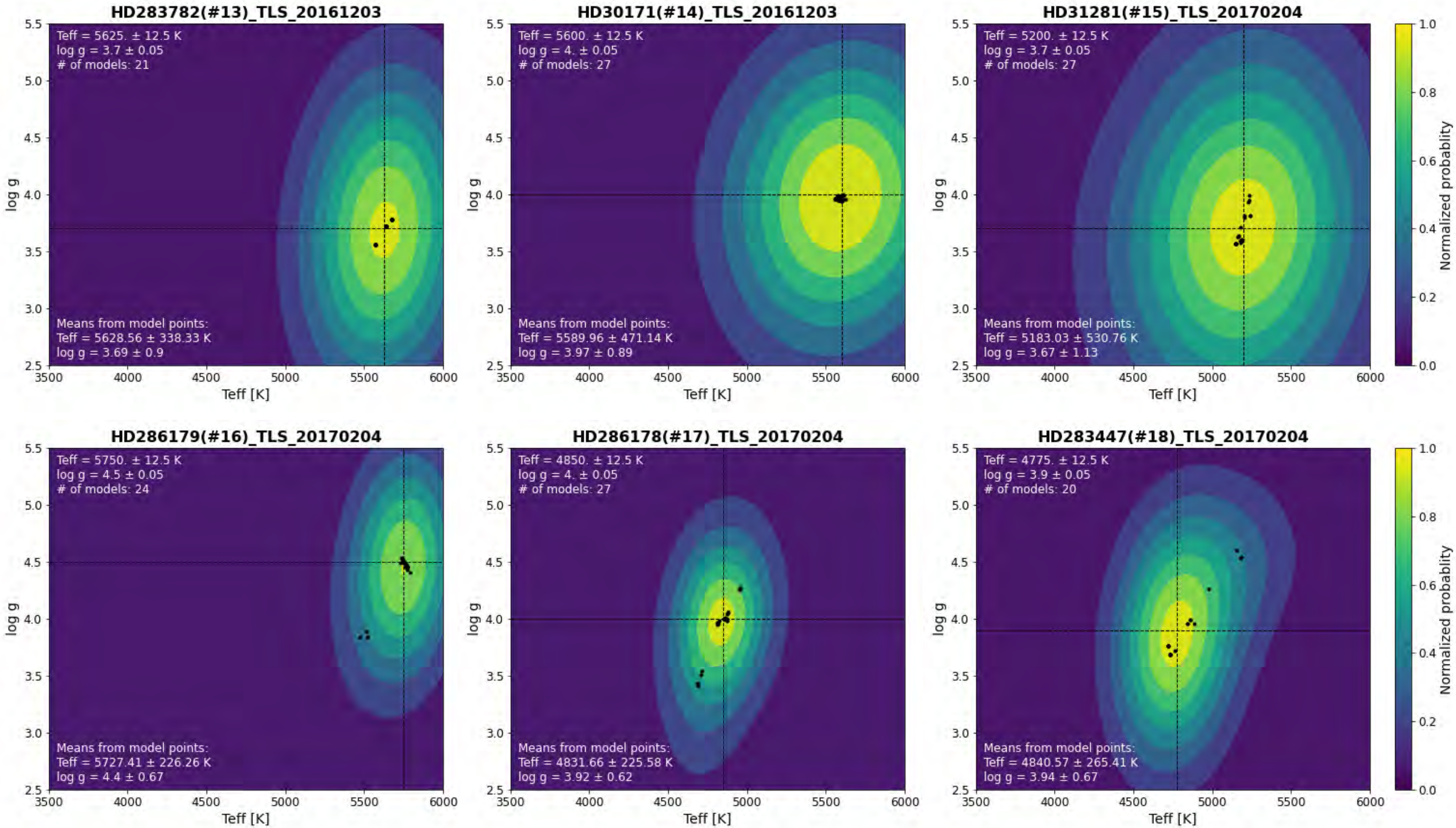

Atmospheric modelling

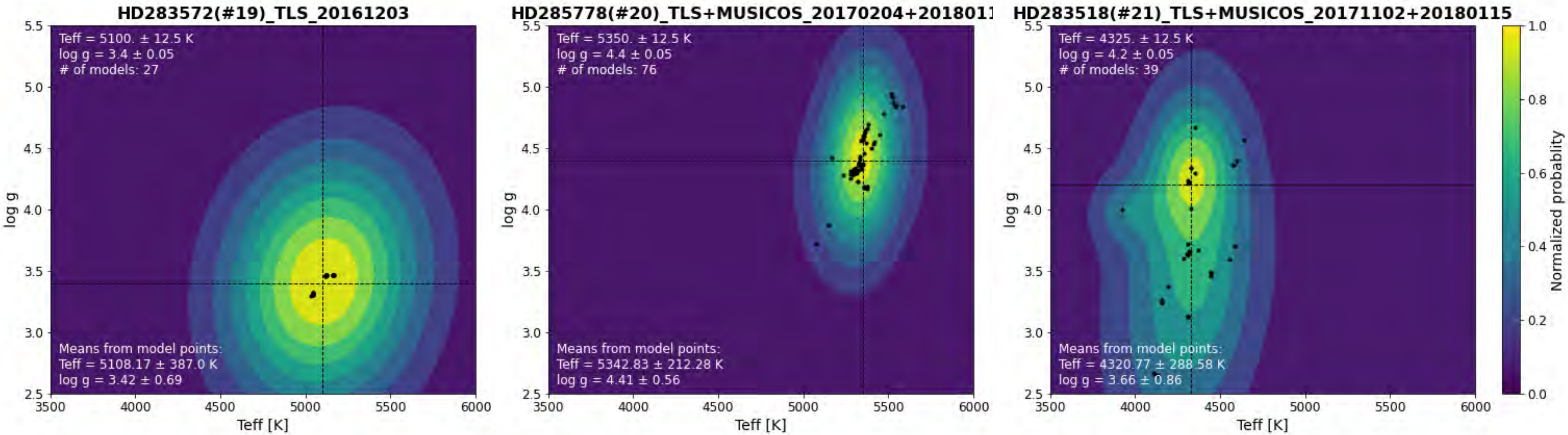

Atmospheric modelling

#	Object name	Strömgren photometry modelling $T_{\rm eff}$ [K]	log g [dex]	[Fe/H] [dex]	Asiago Sp. type	$T_{\rm sp}$ [K]	iSpec atmospheric modelling $T_{\rm eff}$ [K]	log g [dex]	[Fe/H] [dex]
01	HD 285281	4817(557)	4.38(51)	-0.11	K0 V	5150	5146(310)	3.96(66)	-0.33(35)
02	V1298 Tau	5171(151)	4.57(28)	+0.01	K1 V	4980	5163(244)	4.09(45)	+0.01(23)
03	HD 284135	5700(236)	4.08(28)	-0.56	G2 V	5790	5323(359)	3.85(1.08)	-0.74(51)
04	HD 284149	6072(167)	4.16(31)	-0.65	F9 V	6090	5615(292)	4.06(54)	-0.65(56)
05	HD 281691	5158(211)	4.61(26)	+0.19	K0 V	5150	4960(153)	4.10(25)	-0.46(23)
06	HD 284266	5854(234)	4.38(39)	-0.13	G9 V	5230	4974(395)	3.90(70)	-0.77(41)
07	HIP 20782	-	-	-	-	-	5114(342)	3.30(67)	-0.76(34)
08	HD 284503	5427(266)	4.15(39)	-0.23	G2 V	5790	4939(313)	3.78(67)	-0.48(23)
09	HD 284496	5432(95)	4.43(66)	-0.23	G8 V	5310	5294(195)	4.33(41)	-0.19(30)
10	HD 285840	5640(44)	4.45	-	-	-	5272(231)	4.36(38)	-0.30(32)
11	HD 285957	4945(257)	4.79(25)	+0.06	-	-	4729(182)	3.97(31)	-0.78(24)
12	HD 283798	5759(128)	4.69(36)	+0.60	G2 IV	5790	5574(310)	3.90(67)	-0.15(33)
13	HD 283782	4937(660)	4.72(29)	+0.08	G2 IV	5790	5629(338)	3.69(90)	-0.30(64)
14	HD 30171	5390(258)	4.04(51)	-0.35	G3 IV	5710	5590(471)	3.97(89)	-0.35(51)
15	HD 31281	5486(355)	3.97(48)	-0.56	G2 V	5790	5183(531)	3.67(1.13)	-0.79(51)
16	HD 286179	5798(303)	4.63(44)	-0.15	G2 V	5790	5727(226)	4.40(67)	-0.16(22)
17	HD 286178	4490(87)	4.64	-	K0 V	5150	4832(226)	3.92(62)	-0.40(30)
18	HD 283447	4049(55)	4.71	-	K2 V	4830	4841(265)	3.94(67)	-0.14(26)
19	HD 283572	5340(63)	4.51	-	G2 IV	5790	5108(387)	3.42(69)	-0.50(13)
20	HD 285778	5304(254)	4.05(51)	-0.35	G7 V	5390	5343(212)	4.41(56)	-0.34(24)
21	HD 283518	3770	4.78	-	K3 V	4680	4780(335)	3.68(41)	-0.38(39)

Atmospheric modelling

#	Object name	Strömgren photometry modelling $T_{\rm eff}$ [K]	log g [dex]	[Fe/H] [dex]	Asiago Sp. type	$T_{\rm sp}$ [K]	iSpec atmospheric modelling $T_{\rm eff}$ [K]	log g [dex]	[Fe/H] [dex]
01	HD 285281	4817(557)	4.38(51)	-0.11	K0 V	5150	5146(310)	3.96(66)	-0.33(35)
02	V1298 Tau	5171(151)	4.57(28)	+0.01	K1 V	4980	5163(244)	4.09(45)	+0.01(23)
03	HD 284135	5700(236)	4.08(28)	-0.56	G2 V	5790	5323(359)	3.85(1.08)	-0.74(51)
04	HD 284149	6072(167)	4.16(31)	-0.65	F9 V	6090	5615(292)	4.06(54)	-0.65(56)
05	HD 281691	5158(211)	4.61(26)	+0.19	K0 V	5150	4960(153)	4.10(25)	-0.46(23)
06	HD 284266	5854(234)	4.38(39)	-0.13	G9 V	5230	4974(395)	3.90(70)	-0.77(41)
07	HIP 20782	-	-	-	-	-	5114(342)	3.30(67)	-0.76(34)
08	HD 284503	5427(266)	4.15(39)	-0.23	G2 V	5790	4939(313)	3.78(67)	-0.48(23)
09	HD 284496	5432(95)	4.43(66)	-0.23	G8 V	5310	5294(195)	4.33(41)	-0.19(30)
10	HD 285840	5640(44)	4.45	-	-	-	5272(231)	4.36(38)	-0.30(32)
11	HD 285957	4945(257)	4.79(25)	+0.06	-	-	4729(182)	3.97(31)	-0.78(24)
12	HD 283798	5759(128)	4.69(36)	+0.60	G2 IV	5790	5574(310)	3.90(67)	-0.15(33)
13	HD 283782	4937(660)	4.72(29)	+0.08	G2 IV	5790	5629(338)	3.69(90)	-0.30(64)
14	HD 30171	5390(258)	4.04(51)	-0.35	G3 IV	5710	5590(471)	3.97(89)	-0.35(51)
15	HD 31281	5486(355)	3.97(48)	-0.56	G2 V	5790	5183(531)	3.67(1.13)	-0.79(51)
16	HD 286179	5798(303)	4.63(44)	-0.15	G2 V	5790	5727(226)	4.40(67)	-0.16(22)
17	HD 286178	4490(87)	4.64	-	K0 V	5150	4832(226)	3.92(62)	-0.40(30)
18	HD 283447	4049(55)	4.71	-	K2 V	4830	4841(265)	3.94(67)	-0.14(26)
19	HD 283572	5340(63)	4.51	-	G2 IV	5790	5108(387)	3.42(69)	-0.50(13)
20	HD 285778	5304(254)	4.05(51)	-0.35	G7 V	5390	5343(212)	4.41(56)	-0.34(24)
21	HD 283518	3770	4.78	-	K3 V	4680	4780(335)	3.68(41)	-0.38(39)

Evolved post-TTS?

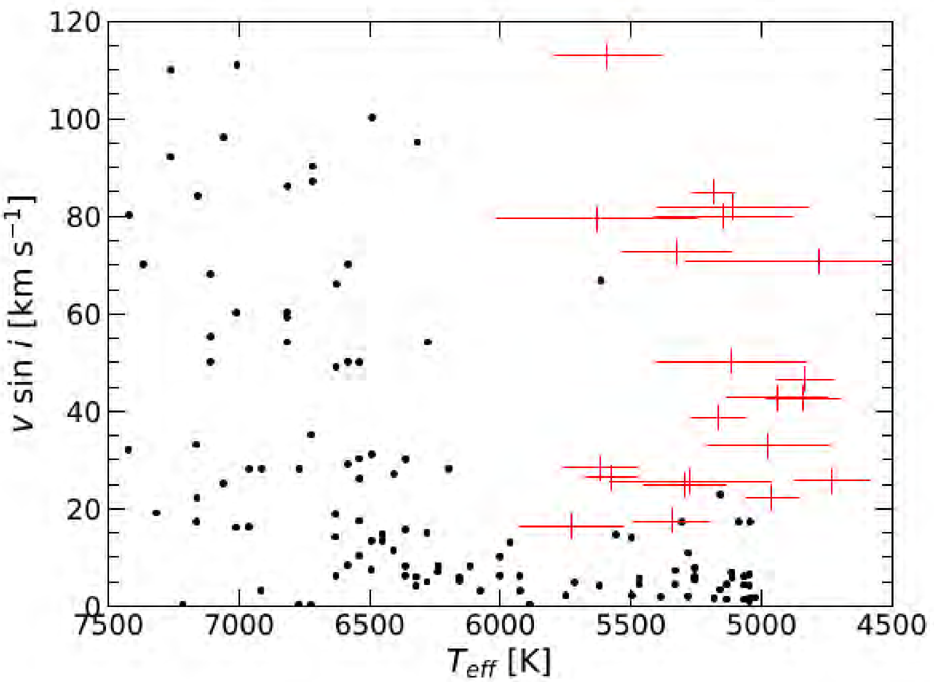

Figure 1. Dependence of the projected rotational velocity, $v \sin i$, on the effective temperature, $T_{\rm eff}$. Black points are data of MS stars from Mallik et al. (2003). Red error bars represent individual targets of this work. Results from `iSpec` modelling were used for the temperature. Rotation was measured from the BF method.

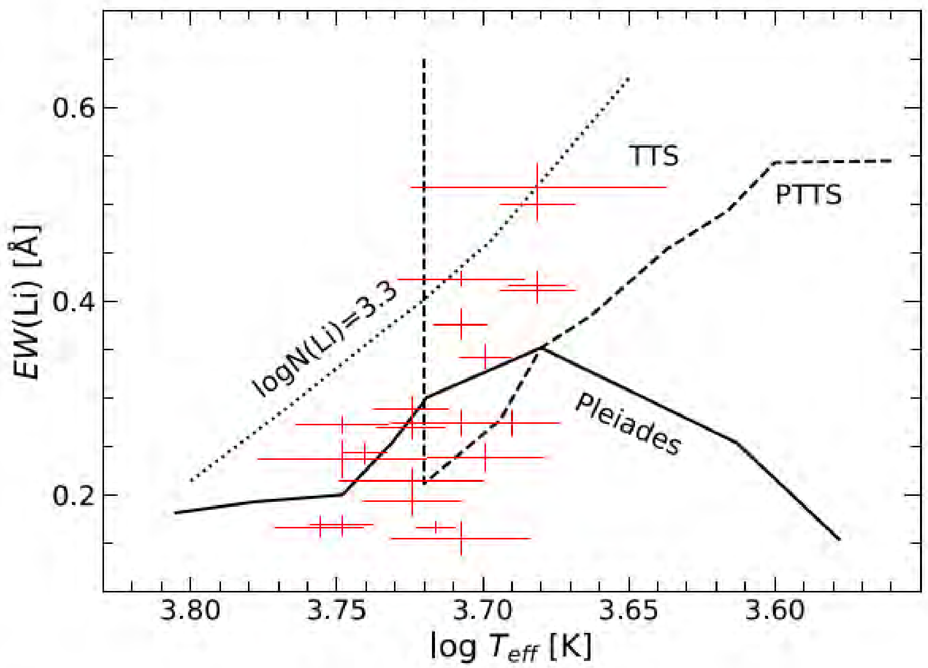

Figure 2. Measured EW of Li I 6708 line as a function of target star temperature as modelled by `iSpec`: Red error bars show individual targets. Underlying figure from Covino et al. (2005), the boundary of post-TTS (PTTS, dashed line) taken from Martin (1997). The solid line shows the upper limit for the Pleiades cluster, while the dotted line indicates the cosmic abundance of lithium.

Reddening

Unreallistic:
- IRSA dust map (full line of sight)

Upper estimate:
- 3D dustmap Bayestar19 by Green et al., 2019

From spectra:
- empirical *E*(B-V) from EW Na I by Poznanski et al., 2012

- comparison by model spectra vs Asiago data

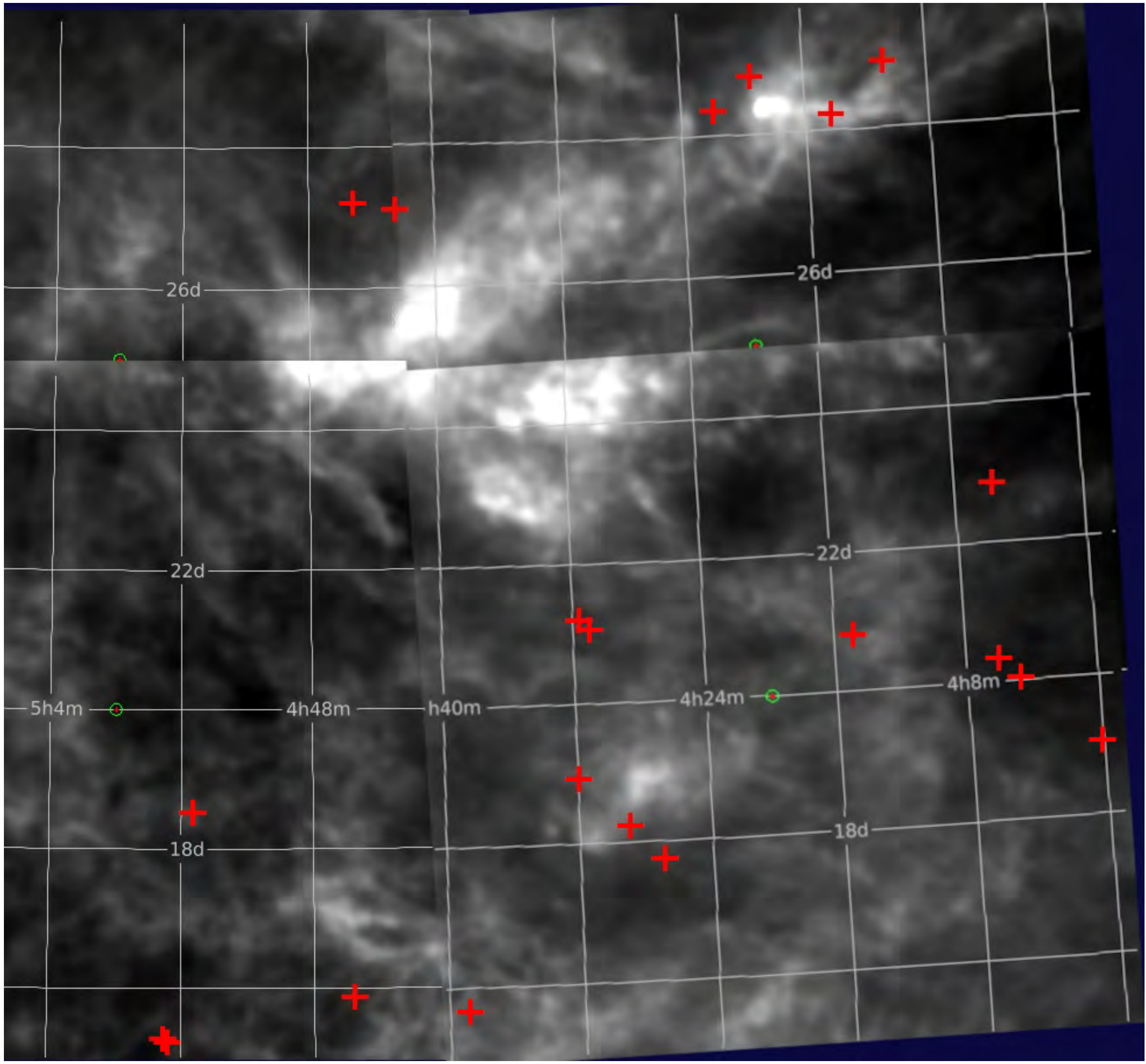

Reddening

Unreallistic:

- IRSA dust map
  (full line of sight)

Upper estimate:

- 3D dustmap Bayestar19
  by Green et al., 2019

From spectra:

- empirical *E*(B-V) from EW Na I
  by Poznanski et al., 2012

- comparison by model
  spectra vs Asiago data

#	Object name	Asiago	Bayestar19	Sodium
01	HD 285281	0.2	< 0.053	0.021(80)
02	V1298 Tau	0.2	< 0.168	–
03	HD 284135	0.0	< 0.027	0.021(80)
04	HD 284149	0.0	< 0.062	0.016(80)
05	HD 281691	0.1	< 0.194	–
06	HD 284266	0.0	< 0.009	0.023(80)
07	HIP 20782	–	< 0.009	0.015(80)
08	HD 284503	0.0	< 0.009	0.016(80)
09	HD 284496	0.1	< 0.018	0.019(80)
10	HD 285840	–	< 0.009	–
11	HD 285957	–	< 0.053	0.018(80)
12	HD 283798	0.0	< 0.044	–
13	HD 283782	0.3	< 0.327	0.027(80)
14	HD 30171	0.1	< 0.062	0.021(80)
15	HD 31281	0.0	< 0.009	0.021(80)
16	HD 286179	0.1	< 0.009	–
17	HD 286178	0.2	< 0.009	0.018(80)
18	HD 283447	0.6	< 0.009	0.028(80)
19	HD 283572	0.0	< 0.009	0.021(80)
20	HD 285778	0.0	< 0.009	–
21	HD 283518	0.3	< 0.044	0.015(80)

Reddening

T_{eff}, $\log g$ by `iSpec`
Reddening law by Cardelli et al., 1989

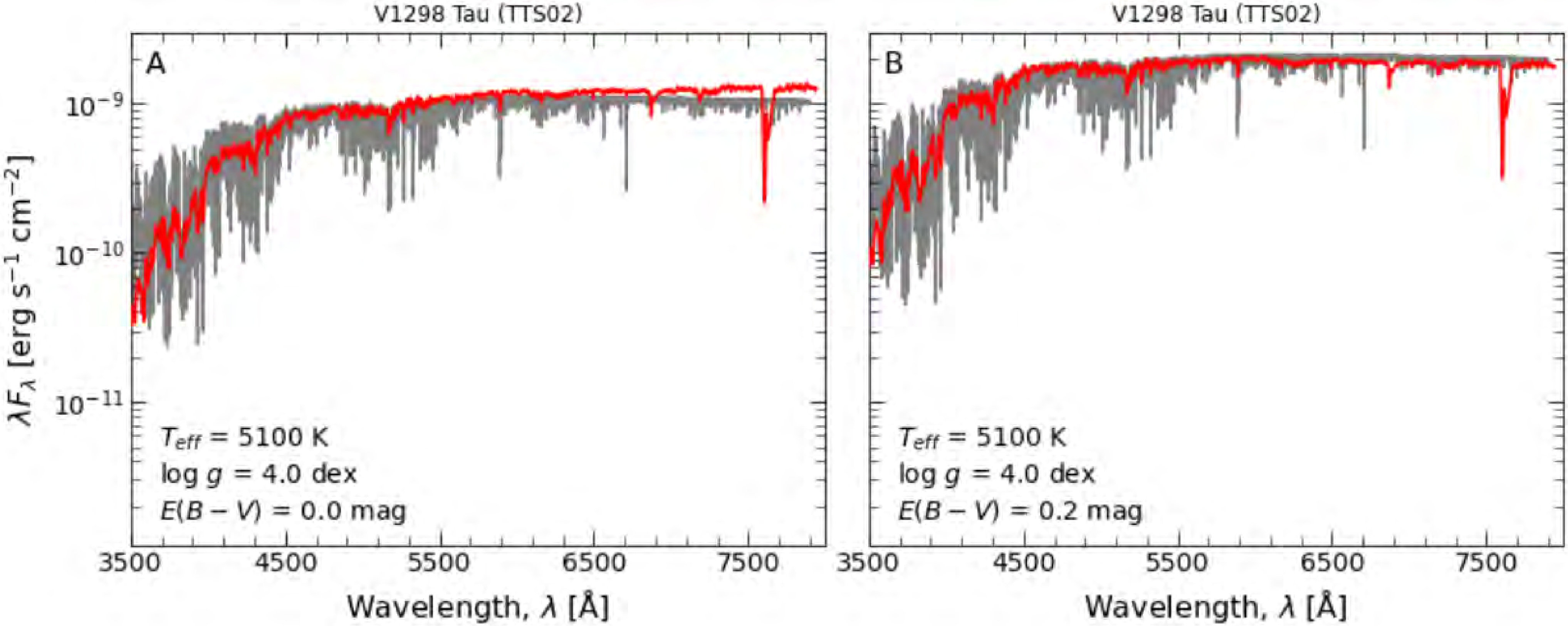

Figure 3. Comparison of low-resolution ASI spectrum of V1298 Tau (red) with PHOENIX model spectrum (black) corresponding to the best-fit **iSpec** result T_{eff} and $\log g$ as indicated on the bottom left pane. Original data (left, panel A) and data de-reddened with $E(B-V) = 0.2$ (right, panel B).

Case of HD 283447

Previous estimates: T_{eff} ~ 4000 K, Our: T_{eff} ~ 4840 K
Multiple ISM?

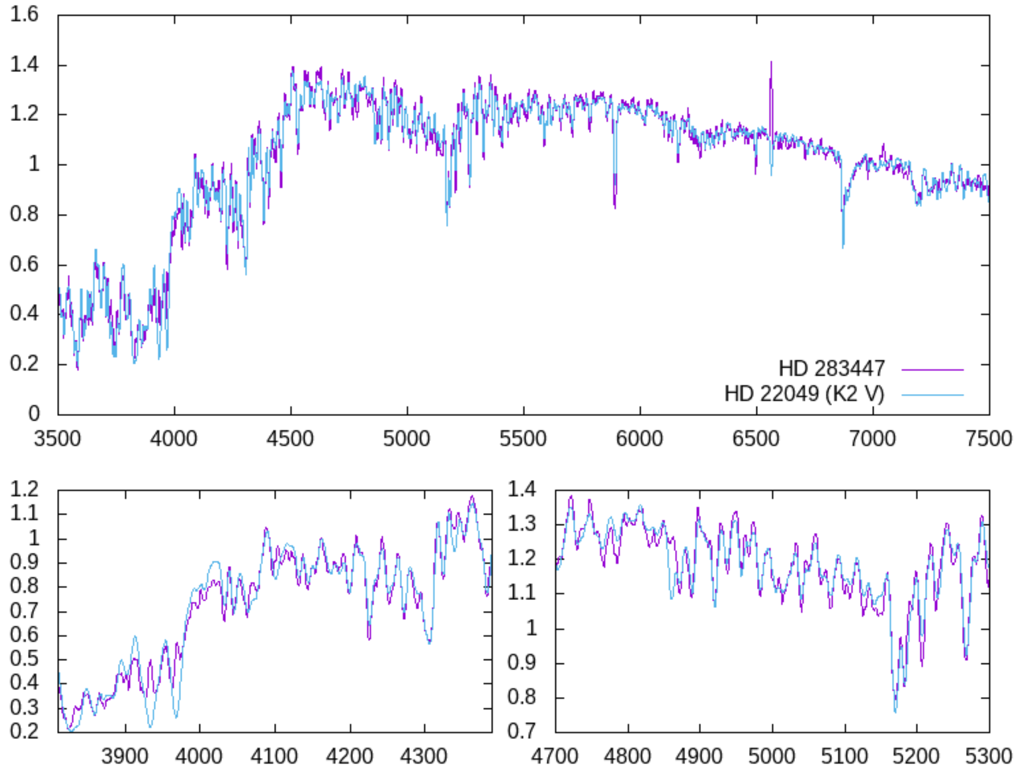

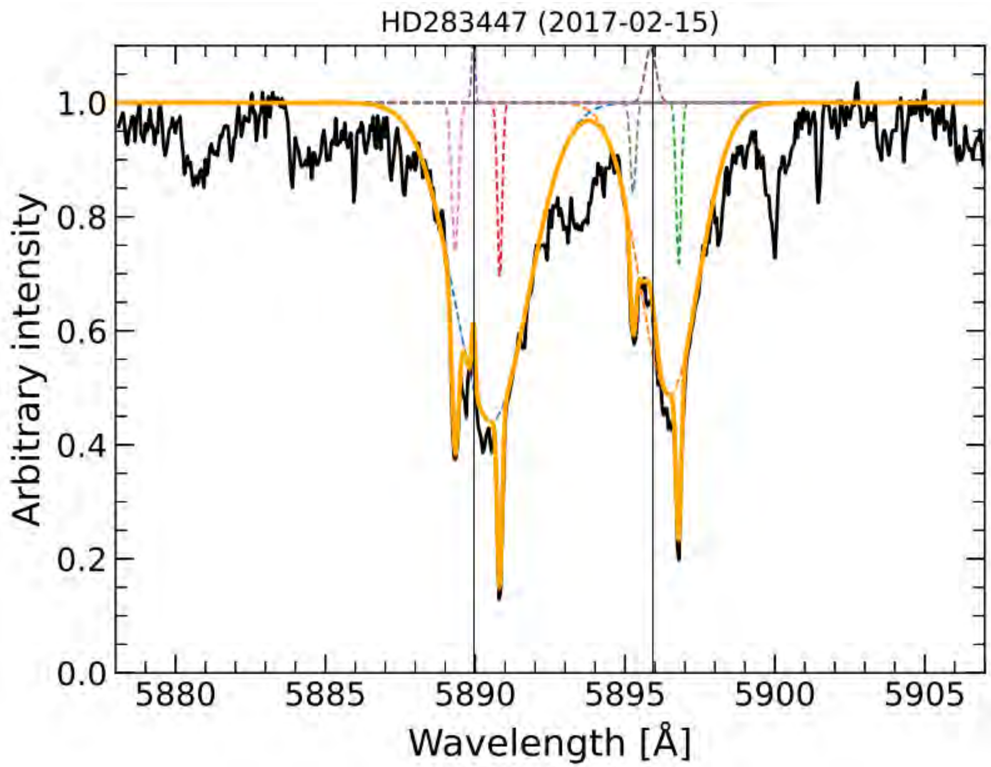

Case of HD 283447

Previous estimates: T_{eff} ~ 4000 K, Our: T_{eff} ~ 4840 K

~~Multiple ISM?~~

Asymetries in RV

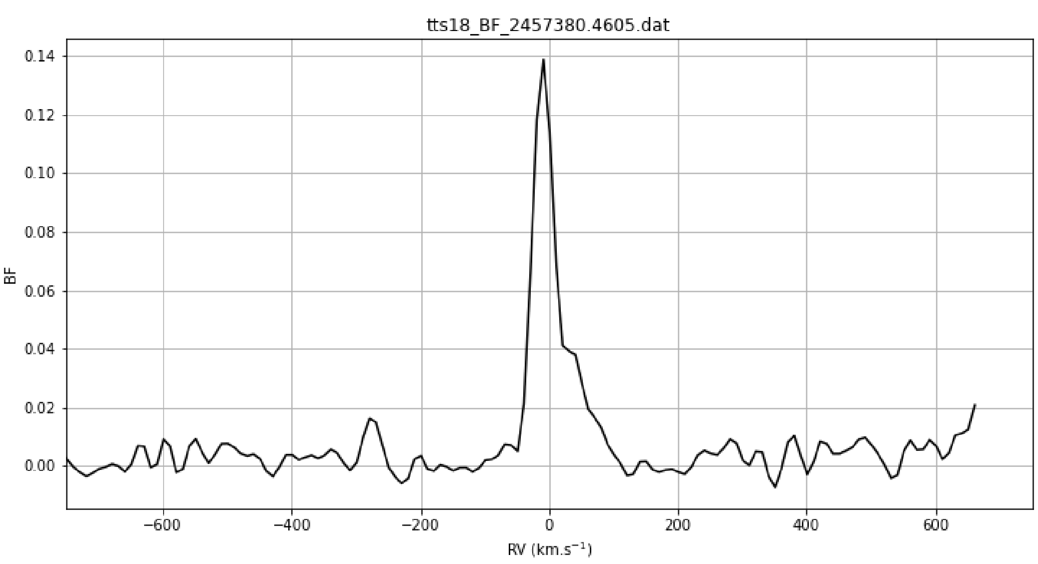

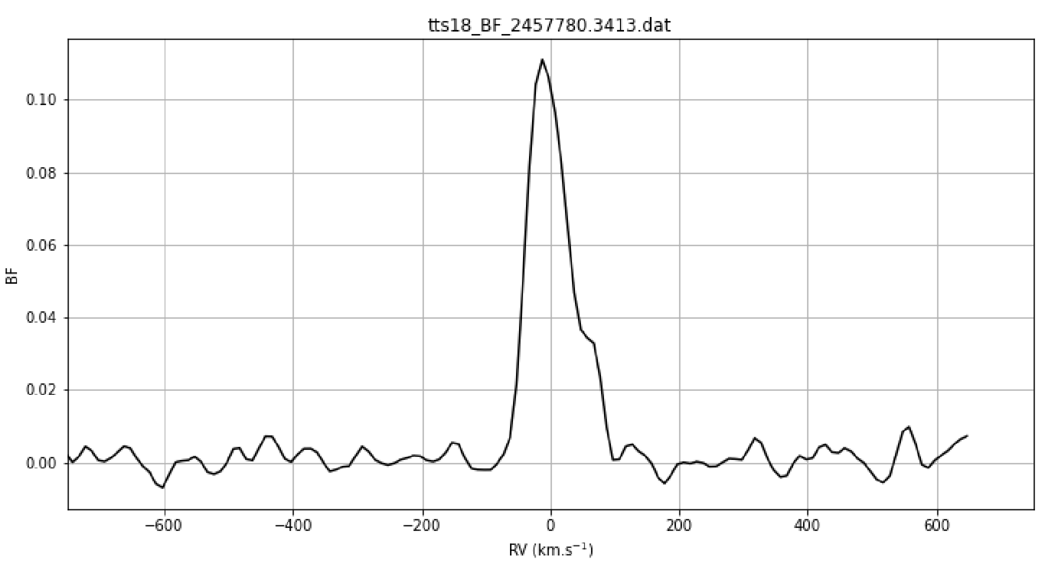

Case of HD 283447

Previous estimates: T_{eff} ~ 4000 K, Our: T_{eff} ~ 4840 K

~~Multiple ISM?~~

Asymetries in RV

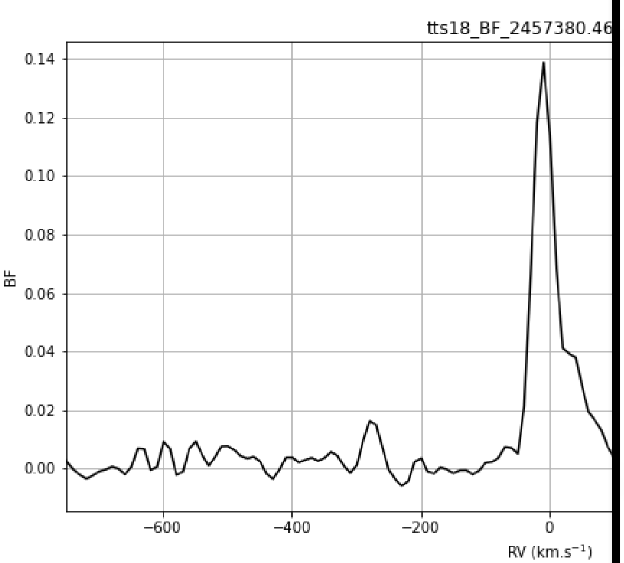

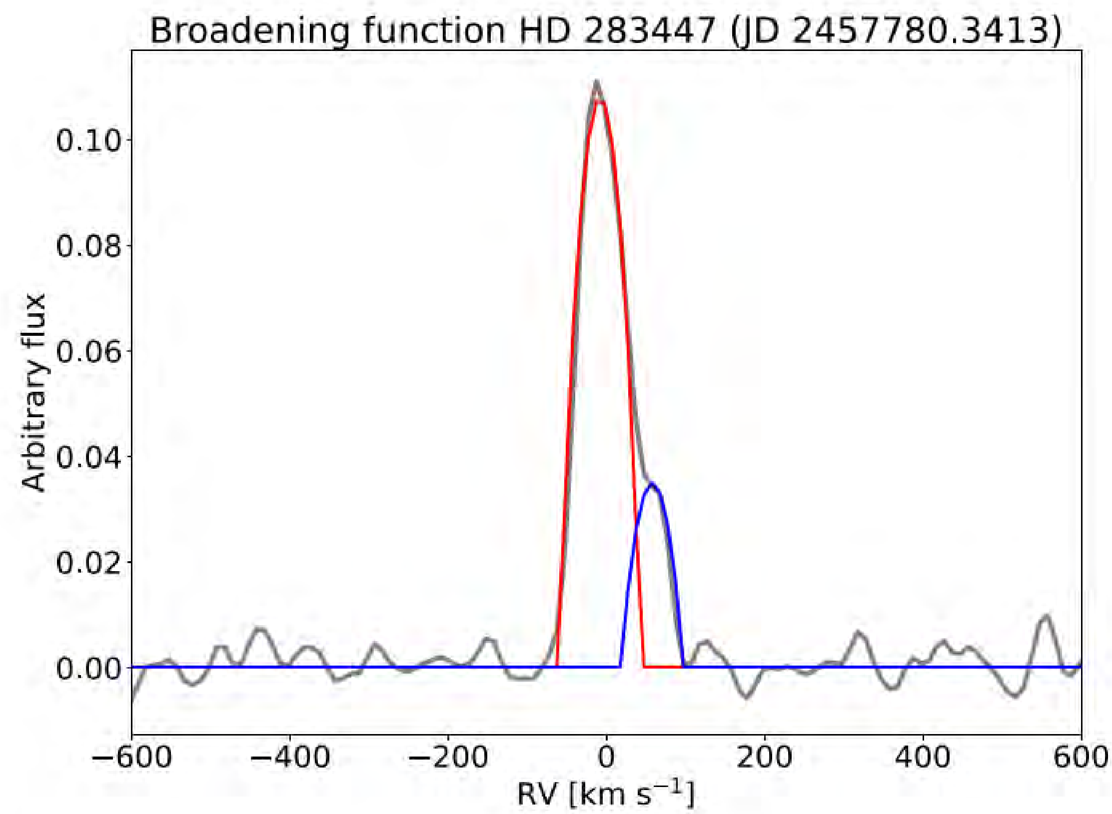

Figure 6. Broadening function plot (grey) of HD 283447 from spectrum acquired on January 26, 2017 at Stará Lesná. Overplotted are two rotational profiles (red and blue solid lines).

Case of HD 283447

Previous estimates: T_{eff} ~ 4000 K, Our: T_{eff} ~ 4840 K

~~Multiple ISM?~~

Asymetries in RV

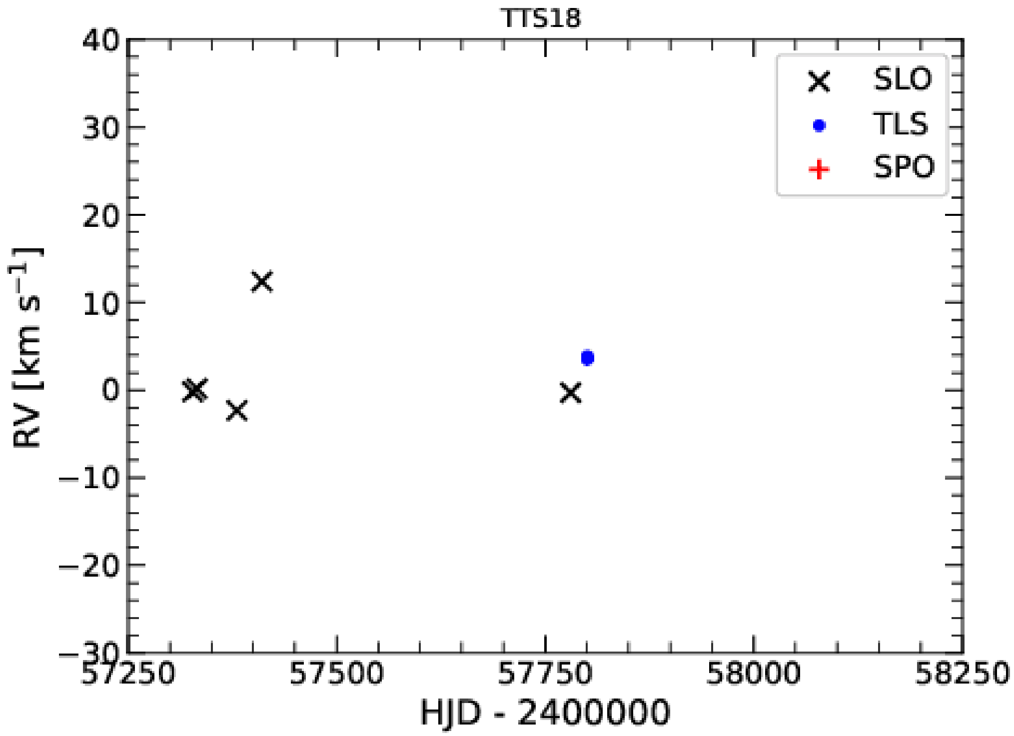

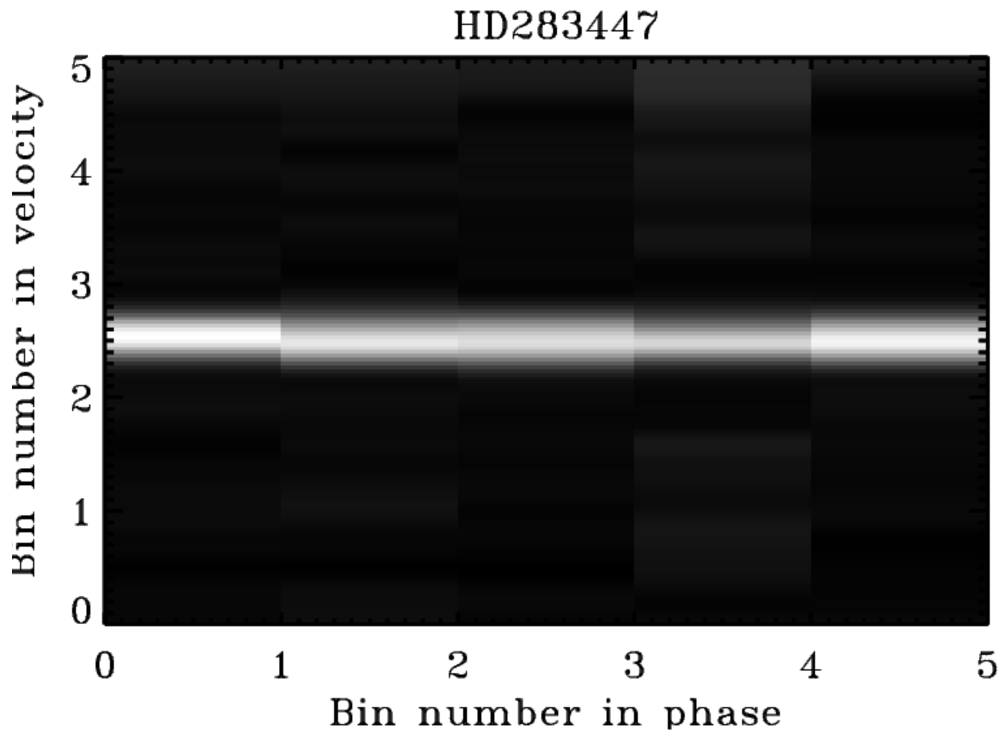

Case of HD 283447

Previous estimates: T_{eff} ~ 4000 K, Our: T_{eff} ~ 4840 K

~~Multiple ISM?~~

Asymetries in RV

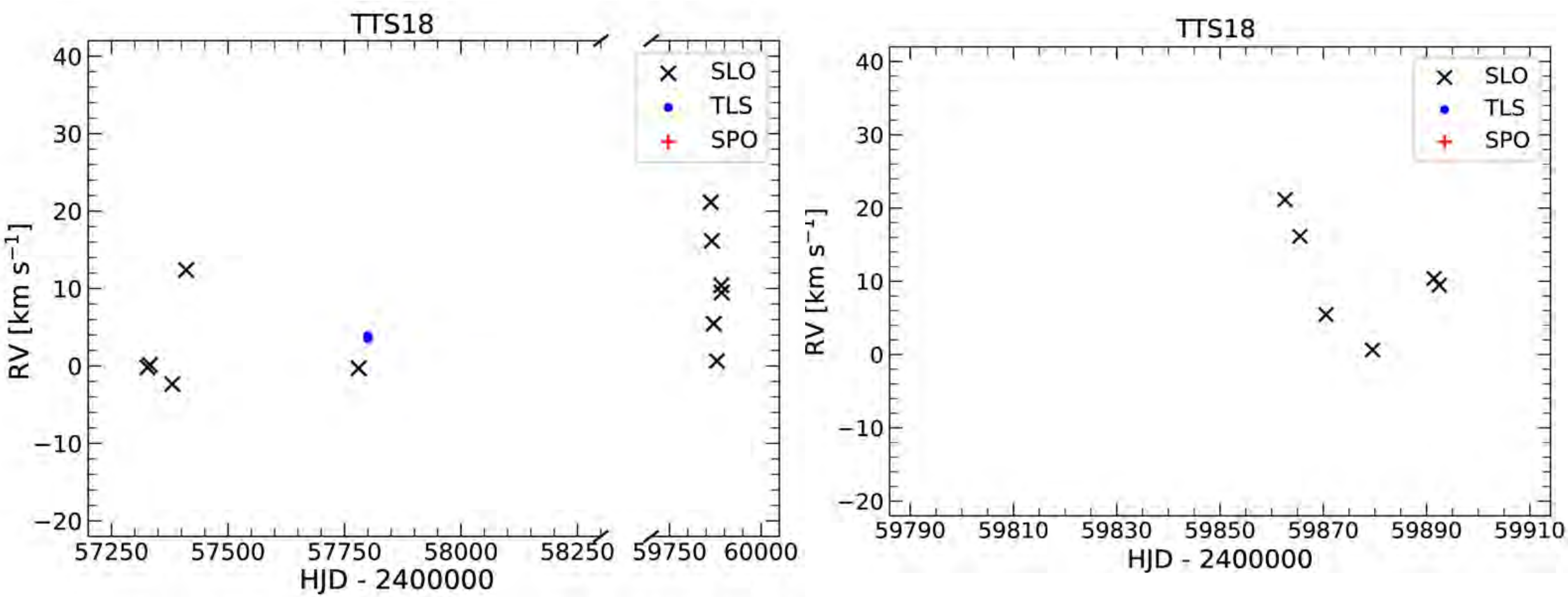

Case of HD 283447

Previous estimates: T_{eff} ~ 4000 K, Our: T_{eff} ~ 4840 K

~~Multiple ISM?~~

Asymetries in RV

Duchêne et al, 2003 – quadruple from adaptive optics

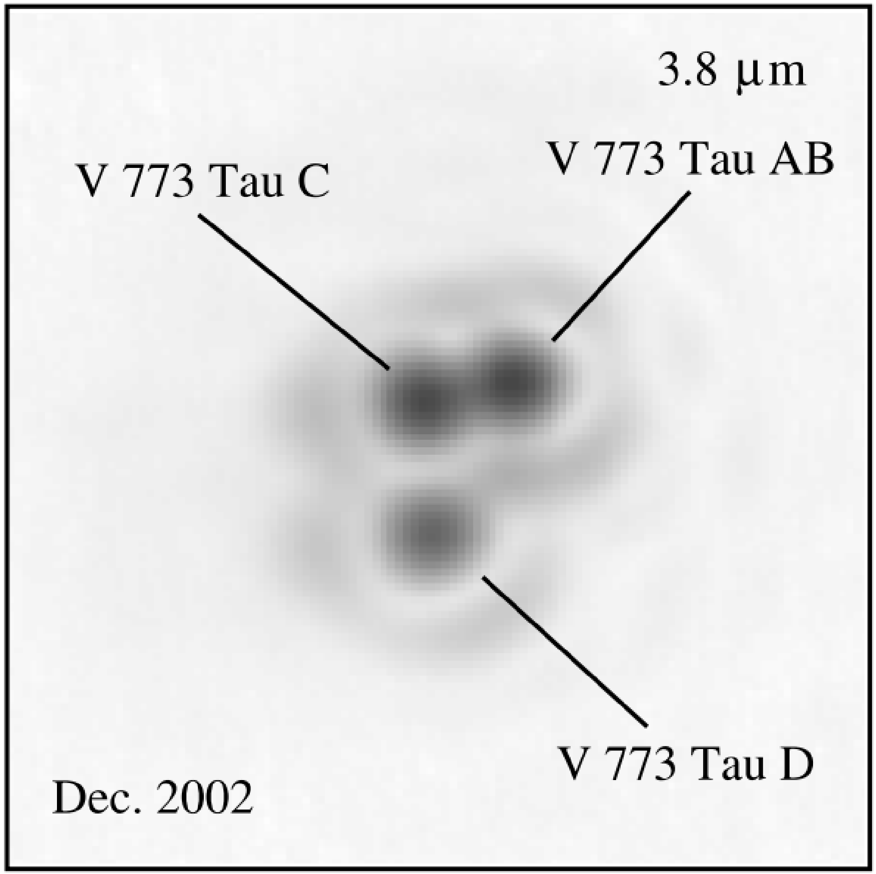

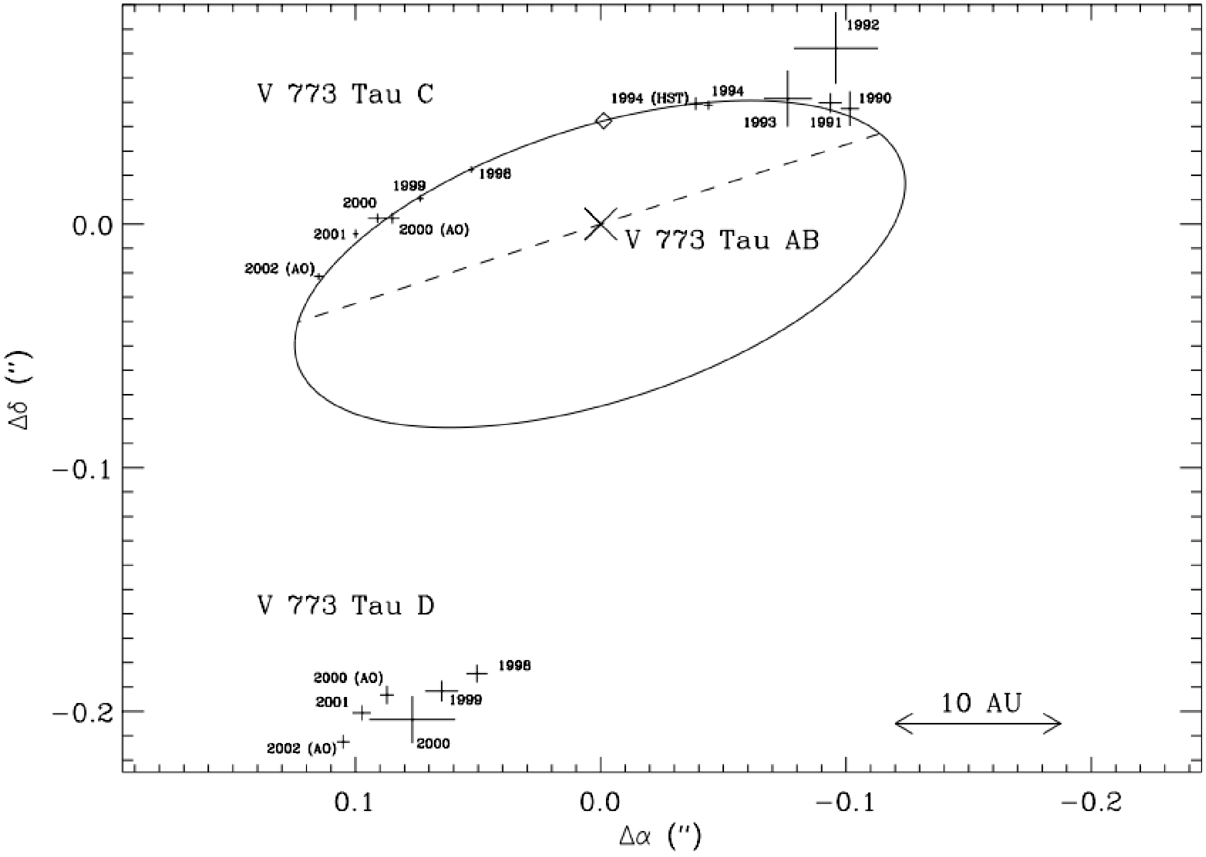

Multiplicity?

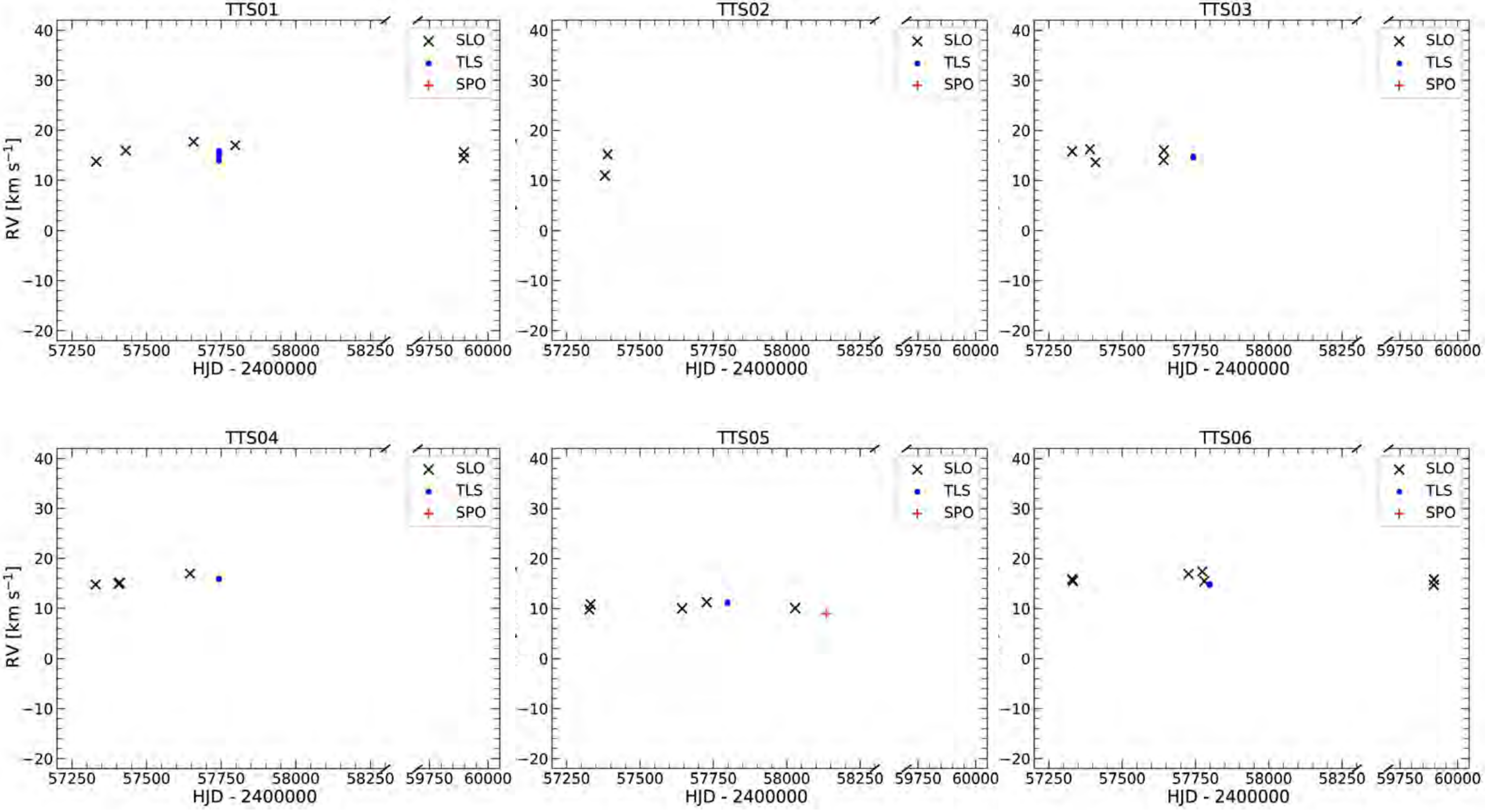

Multiplicity?

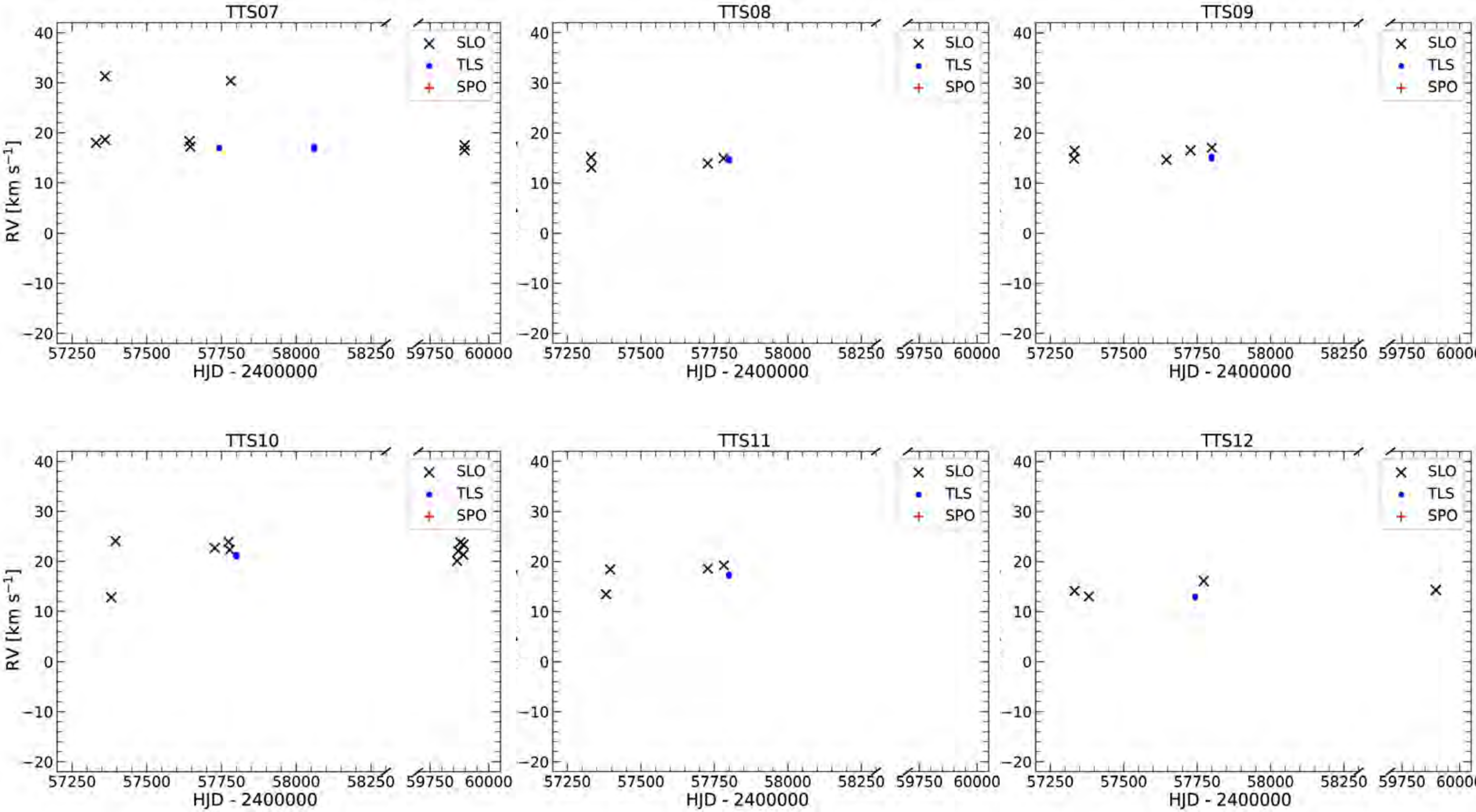

Multiplicity?

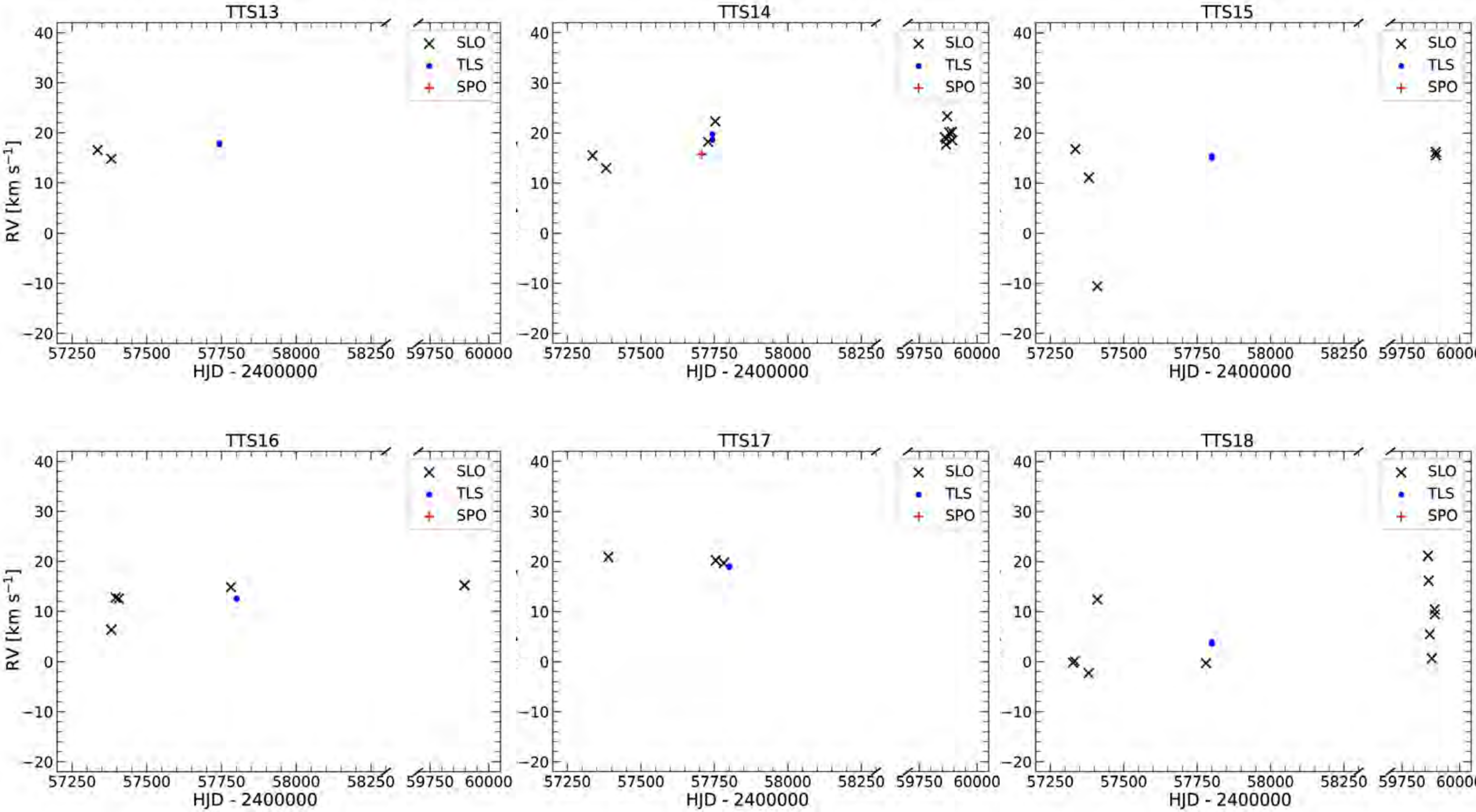

Multiplicity?

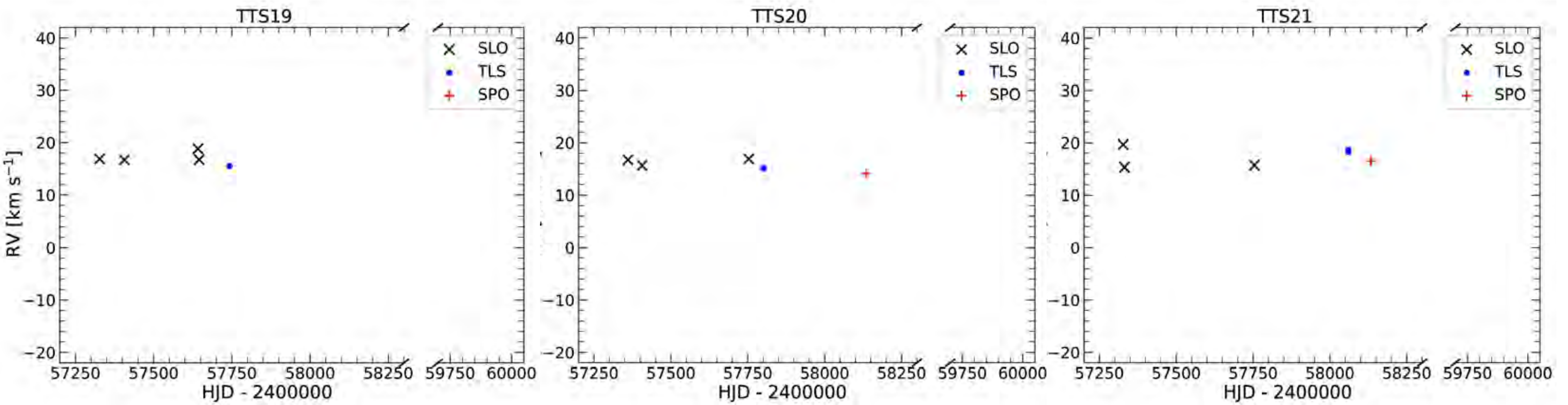

Evolutionary status

Pisa Stellar models (Tognelli et al., 2011) isochrones (Myr) and evolutionary tracks ($M_\odot$)

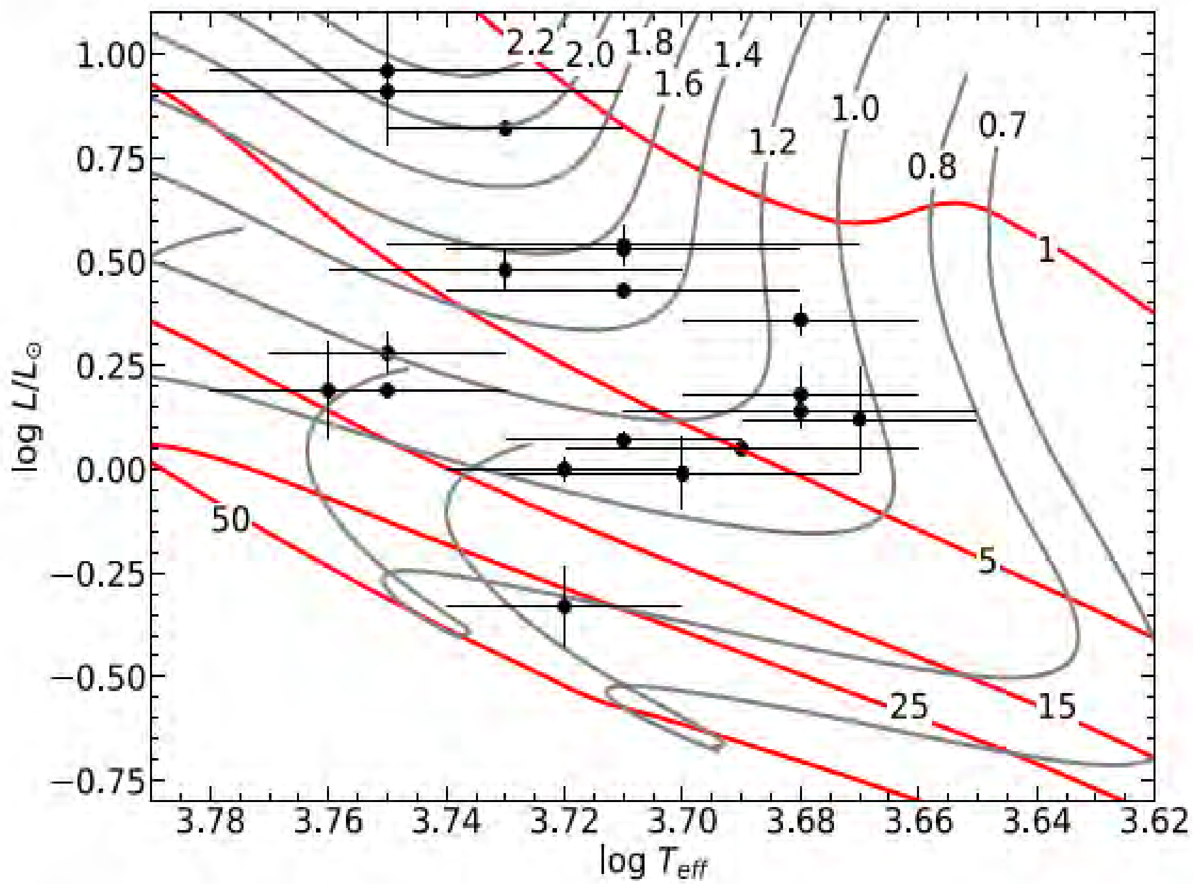

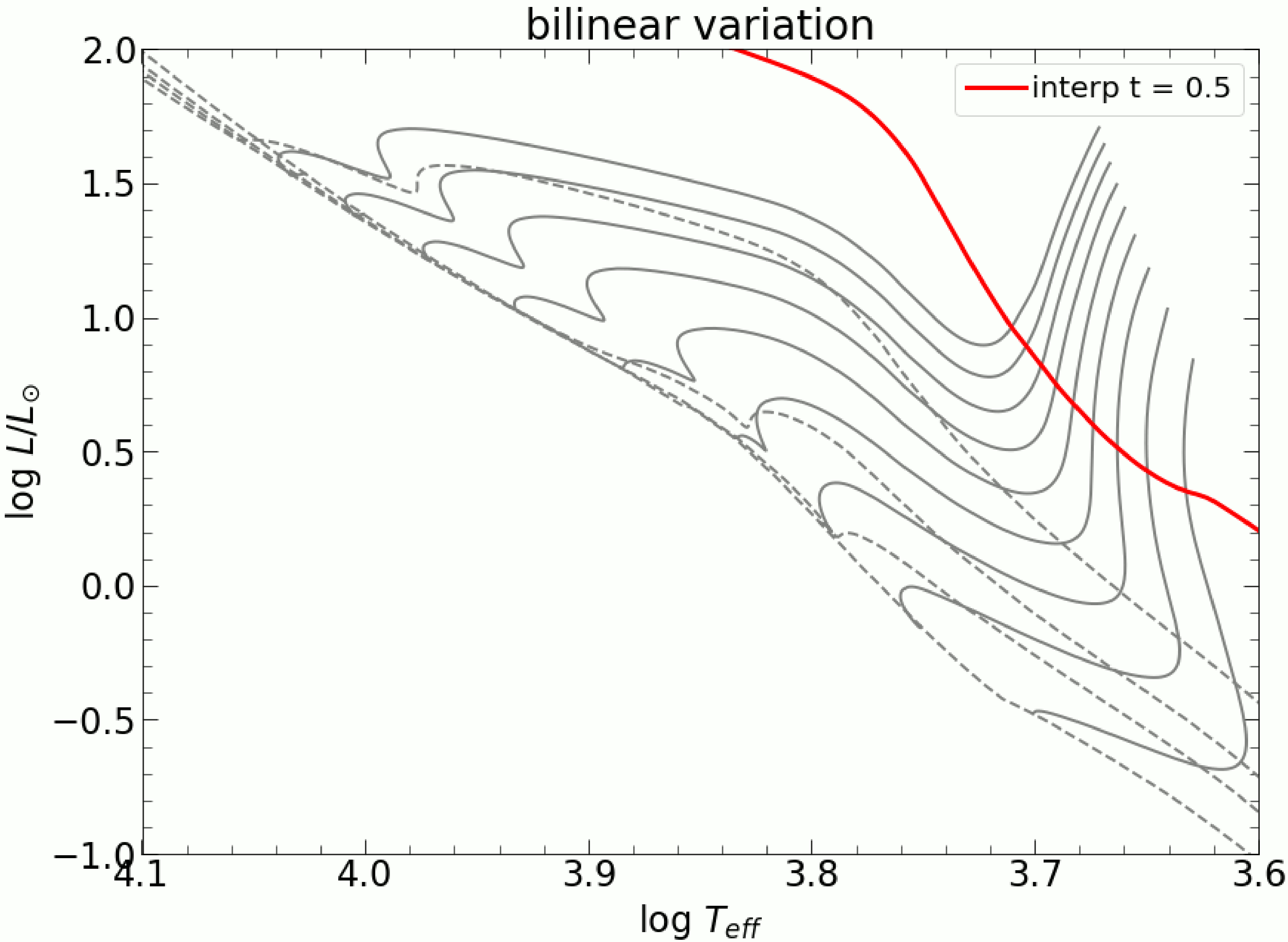
bilinear variation
interp t = 0.5
2.0
1.5
1.0
0.5
0.0
−0.5
−1.0
4.1
4.0
3.9
3.8
3.7
3.6
log $L/L_\odot$
log T_{eff}

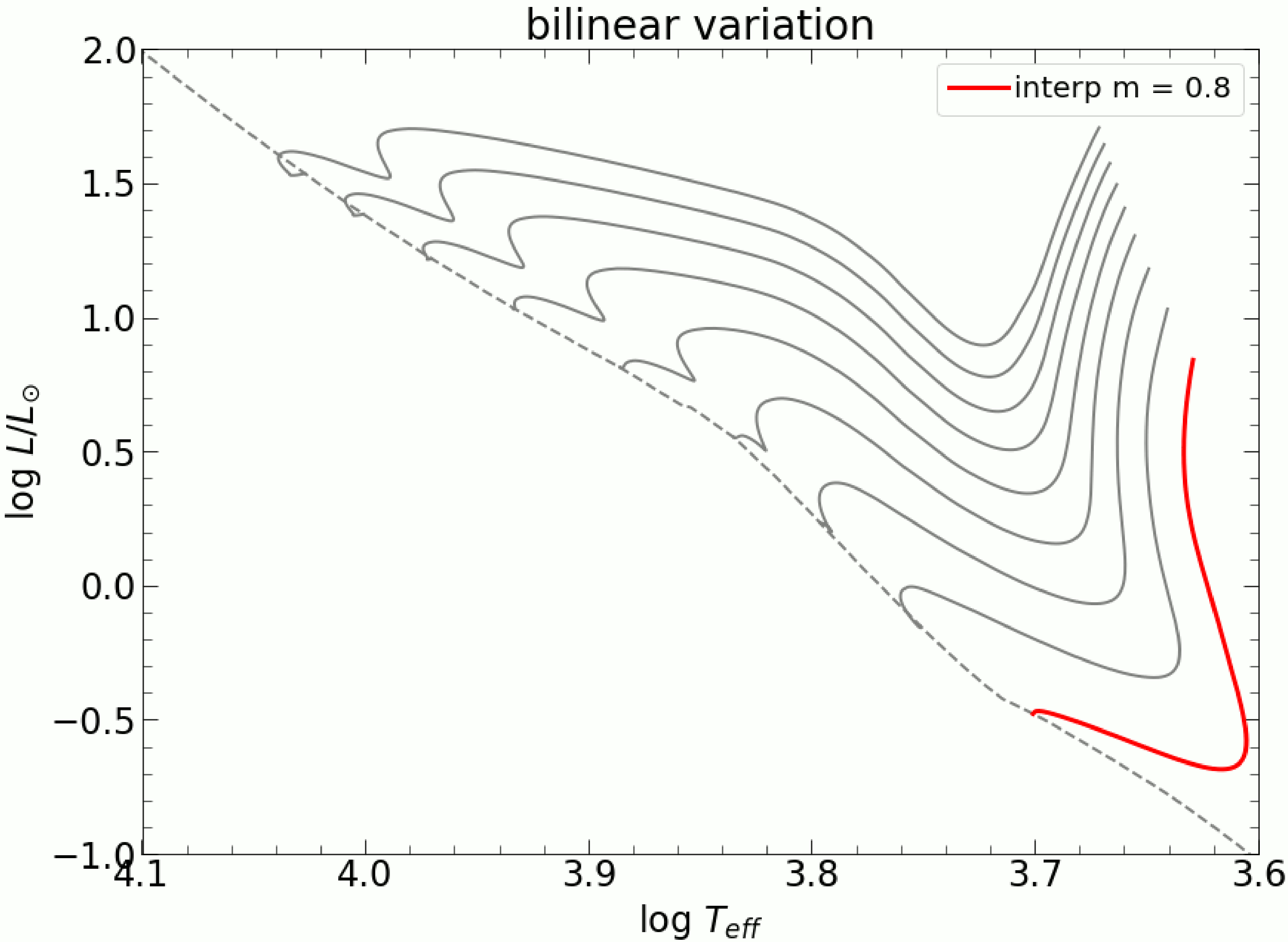
bilinear variation
interp m = 0.8
2.0
1.5
1.0
0.5
0.0
−0.5
−1.0
4.1
4.0
3.9
3.8
3.7
3.6
log $L/L_\odot$
log T_{eff}

Evolutionary status

Pisa Stellar models (Tognelli et al., 201
evolutionary tracks ($M_\odot$)

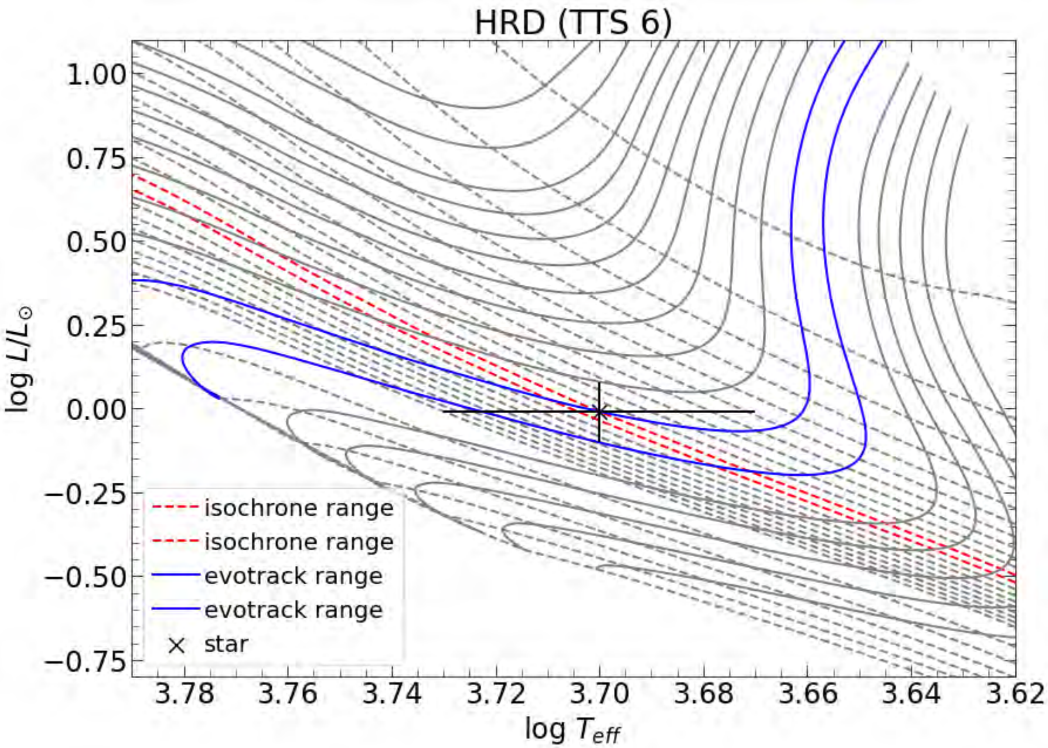

#	Object	$\log T_{\rm eff}$	$\log L/L_\odot$	M [$M_\odot$]	age [Myr]
01	HD 285281	3.71(3)	+0.43(1)	$1.60^{+0.05}_{-0.20}$	4^{+3}_{-2}
02	BD+19 656	3.71(2)	+0.07(2)	$1.25^{+0.10}_{-0.10}$	11^{+5}_{-4}
04	HD 284149	3.75(2)	+0.28(5)	$1.30^{+0.15}_{-0.15}$	13^{+7}_{-4}
05	HD 281691	3.70(1)	−0.01(4)	$1.20^{+0.05}_{-0.05}$	11^{+3}_{-2}
06	HD 284266	3.70(3)	−0.01(9)	$1.20^{+0.15}_{-0.10}$	11^{+9}_{-5}
08	HD 284503	3.69(3)	+0.05(2)	$1.30^{+0.05}_{-0.10}$	7^{+7}_{-4}
09	HD 284496	3.72(2)	+0.00(3)	$1.10^{+0.10}_{-0.05}$	16^{+7}_{-5}
10	HD 285840	3.72(2)	−0.33(10)	$0.85^{+0.05}_{-0.05}$	43^{+7}_{-10}
11	HD 285957	3.67(2)	+0.12(13)	$1.30^{+0.05}_{-0.20}$	4^{+2}_{-2}
12	HD 283798	3.75(2)	+0.19(1)	$1.20^{+0.10}_{-0.10}$	17^{+6}_{-6}
13	HD 283782	3.75(3)	+0.96(18)	$2.20^{+0.30}_{-0.30}$	3^{+2}_{-1}
14	HD 30171	3.75(4)	+0.91(6)	$2.20^{+0.20}_{-0.50}$	3^{+5}_{-1}
15	HD 31281	3.71(4)	+0.54(5)	$1.85^{+0.05}_{-0.50}$	3^{+4}_{-2}
16	HD 286179	3.76(2)	+0.19(12)	$1.15^{+0.10}_{-0.10}$	20^{+5}_{-6}
19	HD 283572	3.71(3)	+0.53(4)	$1.75^{+0.05}_{-0.35}$	3^{+3}_{-2}
20	HD 285778	3.73(2)	+0.82(1)	$2.20^{+0.10}_{-0.20}$	3^{+2}_{-1}
21	HD 283518	3.68(3)	+0.14(4)	$1.35^{+0.15}_{-0.25}$	4^{+4}_{-3}

Radii

$$\log R(L,T) = \frac{1}{2}\left(\log\frac{L}{L_\odot} - 4\log\frac{T_{\rm eff}}{T_{\rm eff,\odot}}\right)$$

$$R\sin i = \frac{P_{\rm rot}\, v\sin i}{2\pi R_\odot}$$

Table 7. Ages and masses from comparing positions in HR diagram to evolutionary PHOENIX models. Distances were set by *Gaia* DR3 parallaxes with reddening inferred from sodium measurement or from the 3D model Bayestar19 (see text). Projected radii calculated from $v\sin i$ and rotation rates from Hambálek et al. (2019). See details on $R(L,T)$ and $R(M,\log g)$ in text. Radii R typeset in *italics* are smaller than minimal $R\sin i$ values.

TTS	Object	$\log T_{\rm eff}$	$\log L/L_\odot$	M [$M_\odot$]	age [Myr]	$R\sin i$ [$R_\odot$]	$R(L,T_i)$ [$R_\odot$]	$R(L,T_A)$ [$R_\odot$]	$R(L,T_G)$ [$R_\odot$]
01	HD 285281	3.711(25)	+0.43(1)	$1.45^{+0.10}_{-0.30}$	3^{+3}_{-2}	1.85	1.92(38)	*1.51(18)*	*1.08(8)*
02	BD+19 656	3.713(20)	+0.07(2)	$1.25^{+0.10}_{-0.10}$	11^{+5}_{-4}	2.18	*1.58(26)*	*1.67(29)*	*1.82(34)*
03	HD 284135	3.726(28)	+0.48(5)	$1.35^{+0.05}_{-0.30}$	2^{+2}_{-1}	1.17	1.80(37)	1.67(27)	–
04	HD 284149	3.749(22)	+0.28(5)	$1.20^{+0.10}_{-0.10}$	9^{+5}_{-3}	0.60	1.16(15)	1.15(11)	1.15(10)
05	HD 281691	3.695(13)	–0.01(4)	$1.10^{+0.05}_{-0.05}$	8^{+2}_{-2}	1.16	1.28(14)	1.22(13)	1.36(13)
06	HD 284266	3.697(33)	–0.01(9)	$0.95^{+0.05}_{-0.15}$	5^{+4}_{-3}	1.20	*0.89(13)*	*1.08(8)*	1.17(8)
08	HD 284503	3.694(27)	+0.05(2)	$1.15^{+0.05}_{-0.20}$	5^{+4}_{-2}	0.62	1.08(13)	0.88(6)	0.91(4)
09	HD 284496	3.724(19)	+0.00(3)	$1.05^{+0.05}_{-0.05}$	11^{+5}_{-4}	1.37	*0.95(8)*	*0.89(6)*	*1.09(5)*
10	HD 285840	3.722(19)	–0.33(10)	$0.80^{+0.05}_{-0.05}$	28^{+12}_{-8}	0.78	1.17(12)	1.40(15)	1.32(9)
11	HD 285957	3.675(16)	+0.12(13)	$0.75^{+0.20}_{-0.20}$	2^{+1}_{-1}	1.57	*1.35(15)*	1.54(18)	*1.34(11)*
12	HD 283798	3.746(24)	+0.19(1)	$1.10^{+0.10}_{-0.10}$	12^{+5}_{-4}	0.51	1.33(19)	1.26(13)	1.39(13)
13	HD 283782	3.750(25)	+0.96(18)	$2.10^{+0.35}_{-0.25}$	3^{+3}_{-2}	3.17	3.28(1.94)	*2.04(63)*	*2.16(67)*
14	HD 30171	3.747(35)	+0.91(6)	$2.10^{+0.10}_{-0.50}$	3^{+4}_{-2}	2.47	2.53(81)	2.15(55)	–
15	HD 31281	3.715(42)	+0.54(5)	$1.20^{+0.25}_{-0.55}$	2^{+1}_{-1}	1.14	1.95(49)	1.62(25)	1.71(25)
16	HD 286179	3.758(17)	+0.19(12)	$1.05^{+0.10}_{-0.10}$	15^{+7}_{-7}	1.02	*0.93(8)*	*0.89(6)*	*0.91(4)*
17	HD 286178	3.684(20)	+0.18(7)	$1.15^{+0.15}_{-0.25}$	3^{+2}_{-1}	1.57	2.39(63)	1.49(20)	–
18	HD 283447	3.685(23)	+0.36(4)	$1.20^{+0.10}_{-0.30}$	2^{+1}_{-1}	2.60	2.51(53)	*1.30(13)*	–
19	HD 283572	3.708(32)	+0.53(4)	$1.55^{+0.10}_{-0.55}$	2^{+2}_{-1}	2.50	2.30(71)	*1.78(33)*	*1.88(34)*
20	HD 285778	3.728(17)	+0.82(1)	$2.00^{+0.05}_{-0.30}$	2^{+1}_{-1}	0.99	1.24(14)	1.05(8)	1.17(6)
21	HD 283518	3.679(29)	+0.14(4)	$1.15^{+0.10}_{-0.35}$	3^{+3}_{-1}	2.62	*2.02(37)*	*1.49(17)*	*1.03(6)*

Note: HD 283447 (TTS 18) is modelled as a single star. However, $\log L/L_\odot$ is contaminated by third light in the system. The minimal radius $R\sin i$ is not affected.

Summary

- 21 WTTS – 178 spectra, computed RV, *v* sin *i*
- 160 spectra used for atmospheric modelling for $T_{\rm eff}$, log *g*, [Fe/H]
- for each mulitple LSQ mininimalization with `iSpec`
- 18 WTTS compared to Asiago spectral atlas, all emission in Ca
- measured EW Li 6104 & 6708 Å for evolution status – 8 stars hot enough for post-TTS
- measured EW of ISM Na doublet for reddening estimation
- found suspected SB1 (TTS14 outside quadruple TTS18) **+** follow-up on targets with changing RVs
- calculated minimum radii *R* sin *i*
- ages and masses from evolutionary models (young, IMTTS, WTTS)

Spectroscopy of selected T Tauri stars

SKALNATÉ PLESO

Thank you !

This work was supported by grants:
APVV-20-0148 and VEGA 2/0031/22

Note on Gaia DR3 solutions

		Strömgren photometry			Asiago		iSpec modelling			*Gaia* DR3 solution		
#	Object name	$T_{\rm eff}$ [K]	log g [dex]	[Fe/H] [dex]	Sp. type	$T_{\rm sp}$ [K]	$T_{\rm eff}$ [K]	log g [dex]	[Fe/H] [dex]	$T_{\rm eff}$ [K]	log g [dex]	[Fe/H] [dex]
01	HD 285281	4817(557)	4.38(51)	-0.11	K0 V	5150	5146(310)	3.96(66)	-0.33(35)	6004(9)	3.89(1)	-0.79(6)
02	V1298 Tau	5171(151)	4.57(28)	+0.01	K1 V	4980	5163(244)	4.09(45)	+0.01(23)	4940(31)	4.22(1)	-0.34(3)
03	HD 284135	5700(236)	4.08(28)	-0.56	G2 V	5790	5323(359)	3.85(1.08)	-0.74(51)	6105(9)	4.21(0)	-0.39(1)
04	HD 284149	6072(167)	4.16(31)	-0.65	F9 V	6090	5615(292)	4.06(54)	-0.65(56)	5035(31)	4.31(1)	-0.52(4)
05	HD 281691	5158(211)	4.61(26)	+0.19	K0 V	5150	4960(153)	4.10(25)	-0.46(23)	5245(46)	4.30(1)	-0.81(6)
06	HD 284266	5854(234)	4.38(39)	-0.13	G9 V	5230	4974(395)	3.90(70)	-0.77(41)	-	-	-
07	HIP 20782	-	-	-	-	-	5114(342)	3.30(67)	-0.76(34)	5801(4)	4.32(0)	-0.32(0)
08	HD 284503	5427(266)	4.15(39)	-0.23	G2 V	5790	4939(313)	3.78(67)	-0.48(23)	6161(86)	3.80(5)	-3.08(66)
09	HD 284496	5432(95)	4.43(66)	-0.23	G8 V	5310	5294(195)	4.33(41)	-0.19(30)	5143(14)	4.33(0)	-0.46(1)
10	HD 285840	5640(44)	4.45	-	-	-	5272(231)	4.36(38)	-0.30(32)	9766(21)	4.06(1)	+0.20(4)
11	HD 285957	4945(257)	4.79(25)	+0.06	-	-	4729(182)	3.97(31)	-0.78(24)	4959(23)	4.13(1)	-0.35(2)
12	HD 283798	5759(128)	4.69(36)	+0.60	G2 IV	5790	5574(310)	3.90(67)	-0.15(33)	5645(23)	4.28(0)	-0.37(2)
13	HD 283782	4937(660)	4.72(29)	+0.08	G2 IV	5790	5629(338)	3.69(90)	-0.30(64)	5752(6)	3.73(1)	-0.01(0)
14	HD 30171	5390(258)	4.04(51)	-0.35	G3 IV	5710	5590(471)	3.97(89)	-0.35(51)	-	-	-
15	HD 31281	5486(355)	3.97(48)	-0.56	G2 V	5790	5183(531)	3.67(1.13)	-0.79(51)	5766(14)	4.11(0)	-0.45(1)
16	HD 286179	5798(303)	4.63(44)	-0.15	G2 V	5790	5727(226)	4.40(67)	-0.16(22)	5842(8)	4.29(0)	-0.35(1)
17	HD 286178	4490(87)	4.64	-	K0 V	5150	4832(226)	3.92(62)	-0.40(30)	-	-	-
18	HD 283447	4049(55)	4.71	-	K2 V	4830	4841(265)	3.94(67)	-0.14(26)	-	-	-
19	HD 283572	5340(63)	4.51	-	G2 IV	5790	5108(387)	3.42(69)	-0.50(13)	5768(3)	3.94(0)	-0.21(0)
20	HD 285778	5304(254)	4.05(51)	-0.35	G7 V	5390	5343(212)	4.41(56)	-0.34(24)	5410(16)	4.27(0)	-0.39(2)
21	HD 283518	3770	4.78	-	K3 V	4680	4780(335)	3.68(41)	-0.38(39)	5353(41)	3.80(1)	-0.41(4)